Accepted Manuscript

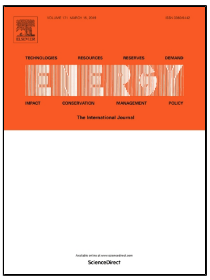

Stochastic Optimization of Trigeneration Systems for Decision-making under Long-term Uncertainty in Energy Demands and Prices

Viviani C. Onishi, Carlos Henggeler Antunes, Eric S. Fraga, Heriberto Cabezas

PII:	S0360-5442(19)30499-2
DOI:	10.1016/j.energy.2019.03.095
Reference:	EGY 14931
To appear in:	*Energy*
Received Date:	03 October 2018
Accepted Date:	17 March 2019

Please cite this article as: Viviani C. Onishi, Carlos Henggeler Antunes, Eric S. Fraga, Heriberto Cabezas, Stochastic Optimization of Trigeneration Systems for Decision-making under Long-term Uncertainty in Energy Demands and Prices, *Energy* (2019), doi: 10.1016/j.energy.2019.03.095

Stochastic Optimization of Trigeneration Systems for Decision-making under Long-term Uncertainty in Energy Demands and Prices

Viviani C. Onishi [a, b, *], Carlos Henggeler Antunes [a, b], Eric S. Fraga [c], Heriberto Cabezas [d]

[a] *Institute for Systems Engineering and Computers at Coimbra – INESC Coimbra, Polo II, Coimbra 3030-290, Portugal*

[b] *Department of Electrical and Computer Engineering, University of Coimbra, Polo II, Coimbra 3030-290, Portugal*

[c] *Centre for Process Systems Engineering, Department of Chemical Engineering, University College London, London WC1E 7JE, UK*

[d] *Institute for Process Systems Engineering and Sustainability, Pazmany Peter Catholic University, Budapest 1088, Hungary*

[*] ***Corresponding author at***. *INESC Coimbra, Department of Electrical and Computer Engineering, University of Coimbra, Polo II, Coimbra 3030-290, Portugal. E-mail addresses: viviani@deec.uc.pt; viviani@inescc.pt; (Viviani C. Onishi).*

ABSTRACT

Combined heating, cooling and power (CHCP) systems, so-called trigeneration, are widely accepted as more energy-efficient and environment-friendly alternatives to traditional separate energy generation. Nevertheless, the tasks of synthesis and optimization of trigeneration systems are strongly hampered by the long-term uncertainties in energy demands and prices. In this work, we introduce a new scenario-based model for the stochastic optimization of CHCP systems under uncertainty in several process design parameters. Energy generation operators are proposed to ensure the optimal sizing and operation of each equipment in each optimization scenario. Our main objective is to enhance energy efficiency by synthesizing the most cost-effective CHCP system able to operate in wide-ranging scenarios of energy demands and prices. For this purpose, uncertain design parameters are modelled as a set of loading and pricing scenarios with given probability of occurrence. The set of scenarios contains correlated energy prices described through a multivariate Normal distribution, which are generated via a Monte Carlo sampling technique with symmetric correlation matrix. The resulting stochastic multiscenario MINLP model is solved to global optimality by minimizing the expected total annualized cost. A thorough economic risk analysis underlines the effectiveness of the proposed methodology. This systematic approach represents a useful tool to support the decision-making process regarding system efficiency and robustness.

Keywords: Mixed-integer nonlinear programming (MINLP); Combined heating, cooling and power (CHCP) production; Integrated sizing and operation; Correlated data uncertainty; Risk management.

1. Introduction

Combined heating, cooling and power (CHCP) production through trigeneration systems has gained considerable traction during the last decade due to its multiple advantages and timeliness. Energy efficiency is a flagship of the European Union for the reduction of greenhouse gas emissions, climate change mitigation, and lessening of primary energy consumption and energy imports. In this light, CHCP systems provide a reliable highly energy-efficient solution to address those challenges. Converting around 75–80% of fuel sources into useful energy and reducing grid losses in comparison to conventional separate production, CHCP systems have the ability to meet thermal and power demands through centralized or distributed energy generation [1,2]. In fact, the European Union has strongly encouraged the assessment of the potential of cogeneration (or combined heating and power – CHP) and trigeneration towards their broad implementation into the residential, commercial and services sectors of the member states [3]. A comprehensive overview on drivers and definitions, along with the major economic, environmental and technological advantages of trigeneration systems is presented in Ref. [4].

The optimal design of CHCP systems can be a complex endeavour. In addition to dealing with different energy demands (heating, cooling and electricity) and available energy technologies, the tasks of synthesis and optimization must also account for uncertainties arising from different sources [5–7]. In CHCP systems design, uncertainties encompass intrinsic long-term fluctuations over the plant lifetime in energy demands, fuel and electricity prices, as well as energy regulations, to list but a few [8,9]. Disregarding uncertainty effects on the system design and operation could lead to suboptimal solutions, in which the impaired economic and energy performances would not provide longstanding economic viability nor reduce financial risks. Nevertheless, most of the research about the optimal design of cogeneration and polygeneration systems still relies

on deterministic approaches that cannot capture the stochastic nature of uncertain design parameters [1,2,10–15].

Gamou et al. [16] have pioneered the use of continuous random variables in stochastic optimization of cogeneration systems, to describe the stochastic behaviour of uncertain energy demands. To do so, the authors have applied a sensitivity analysis and an enumeration methodology, which revealed that hourly energy loads can be portrayed by a Normal distribution with 95% of its area falling in the ±20% average energy demands range. A hierarchical optimization algorithm was then proposed to determine the optimal sizing problem (upper level) and optimal operating planning (lower level). A related stochastic approach has been pursued by Li et al. [17] to address the optimization of building CHCP systems under demand uncertainty. Their approach combines Monte-Carlo simulation method and mixed-integer nonlinear programming (MINLP) optimization. Hu and Cho [18] have also studied the optimization of CHCP systems under uncertainty in the energy demand. The authors have introduced a probability constrained multi-objective programming model, wherein probability constraints are used to ensure that the operational reliability complies with the stochastic energy demand.

Wang and Singh [19] have developed a stochastic multi-objective approach for the optimal economic dispatch of CHP systems. The authors have used a particle swarm optimization (PSO) algorithm to solve the dispatch problem, while treating electric power and heating demands as random decision variables. Ersoz and Colak [20] have investigated the effects of long-term economic uncertainties on the operational planning of industrial CHCP plants. The authors have employed a genetic algorithm (GA) and a non-parametric stochastic approach to improve decision-making process at the investment level. Even if metaheuristic algorithms such as PSO and GA present a number of advantages, their inability to ensure global (or even local, in some cases) optimal

solutions can be a major shortfall in comparison to mathematical programming approaches.

Urbanucci and Testi [8] have proposed a two-stage stochastic model for the optimal sizing and operation of cogeneration systems, considering the long-term uncertainty in energy load demand. Firstly, the authors have employed a probabilistic approach based on a dynamic Monte Carlo simulation of the entire life-cycle of the CHP system for a more comprehensive risk analysis. Then, multi-objective optimization has been performed taking into consideration the operational strategies of *Following the electric load* (FEL) and *Following the thermal load* (FTL). Their results have showed that optimal size and total annual cost savings are significantly impacted by the demand uncertainty. Interestingly, the authors report that the optimal sizing solutions obtained through the probabilistic approach can be up to 30% smaller than those provided by the deterministic one. Yet, it should be noted that the rule-based operating FEL and FTL strategies underperform the results attainable by optimization models [15,18]. Finally, the same authors have emphasized that further research should focus on more complex polygeneration systems with thermal storage, as well as the influence of uncertainty on multiple process parameters, and assessment of correlations between the uncertain parameters. Their suggestion is aligned with the limitations of the aforementioned works, given that generally only a small set of the most important uncertain parameters are considered (*e.g.*, uncertainty in energy demands while neglecting energy prices and their potential correlations).

To overcome shortcomings in preceding research, we introduce a new scenario-based modelling approach for the synthesis and optimization of CHCP systems under long-term uncertainty in energy load demands and prices. Our economic-oriented optimization model is based upon a general superstructure encompassing distinct

equipment units for heating, cooling and electricity generation, along with thermal energy storage and bidirectional grid connection. The methodology combines mathematical programming and stochastic optimization aimed at enhancing process energy efficiency, while accounting for wide-ranging scenarios of energy demands and prices. For this purpose, uncertain design parameters are mathematically modelled as a set of different scenarios with a given probability of occurrence. To the best of our knowledge, this is the first stochastic MINLP-based CHCP model to simultaneously deal with the energy demands uncertainty and the correlation between uncertain energy prices within a multiscenario optimization approach. The resulting stochastic MINLP model is solved to global optimality through the minimization of the expected value for the total annualized cost distribution. An illustrative case study based on a hotel complex in the northern region of Portugal is performed to evaluate the capabilities of the proposed approach. Major contributions and innovative features from this work include:

(i) The development of a stochastic modelling approach for the cost-effective optimization of the integrated sizing and operation of CHCP systems under uncertainty, which can be efficiently solved to global optimality by using state-of-the-art MINLP solvers.

(ii) The proposition of new energy generation operators to ensure the optimal design and operation (on/off status) of each equipment in the entire set of optimization scenarios.

(iii) The consideration of all relevant long-term uncertainty sources that can affect the system performance, which comprise heating, cooling and power demands as well as electricity and natural gas prices.

(iv) The consideration of energy prices as correlated uncertain design parameters, which are generated from a multivariate Normal probability

distribution via Monte Carlo sampling technique based on a symmetric correlation matrix.

(v) The proposition of a scenario generation framework to obtain a set of uncertain probabilistic scenarios that appropriately describe the uncertain search space within a reduced number of scenarios.

(vi) The comprehensive analysis of stochastic solutions in contrast to those obtained from the conventional deterministic approach to demonstrate the inaccuracy of the deterministic CHCP system design.

(vii) The in-depth financial risk analysis to support the long-term decision-making process.

The paper is structured as follows: In **Section 2**, we briefly introduce the problem statement of optimal design and operation of CHCP systems under long-term uncertainty in energy demands and prices. In **Section 3**, we present the proposed methodology regarding the general superstructure definition, scenarios generation framework and optimization strategy. The stochastic and deterministic modelling approaches are developed in **Section 4**. In **Section 5**, we describe the illustrative case study used to assess the accurateness of the new optimization method. The financial risk analysis and critical appraisal of the uncertain parameters influence on the system cost-efficiency are discussed in **Section 6**. Finally, in the last section, we summarize the main remarks and conclusions from this study and provide some directions for future research.

2. Problem statement

The problem of synthesis and optimization of trigeneration (CHCP) systems under long-term uncertainty in both energy load demands and prices can be formally stated as follows. A set of utility streams and energy services (including cooling water, natural gas

and electric power) is given with their related costs. In addition, distinct equipment pieces are considered for heating, cooling and electricity generation as well as energy storage, which include natural gas-fired cogeneration units (reciprocating internal combustion engines – ICEs), auxiliary gas-fired boilers (GFBs), absorption chillers (ACHs), and a thermal energy storage (TES) tank. All equipment units are provided with known technological characteristics (*i.e.*, part-load performance curves, rated capacities and nominal efficiencies) and corresponding capital, operating and maintenance (O&M) costs. Our main goal is to synthesize the most cost-effective CHCP system able to meet end-users thermal and electricity demands, while accounting for a large range of different scenarios of energy loads and prices. Thus, we consider the heating, cooling and electricity demands along with electricity tariffs and fuel prices as uncertain design parameters. The latter are systematically expressed by means of correlated optimization scenarios with distinctive loading and pricing alternatives –hereafter, referred to as loading and pricing (L&P) scenarios–. It is worth mentioning that the uncertainty sources are associated with the significant fluctuations observed in energy demands and energy prices over the lifetime of trigeneration systems. **Fig. 1** displays the general superstructure and the main decision variables proposed for the optimal synthesis, design and operation of CHCP systems.

The simultaneous synthesis (equipment selection) and optimization (equipment sizing and selection of on/off operating status and partial thermal load) of CHCP systems under several sources of uncertainty is a complex task aimed at attaining an optimal plant configuration and operational scheduling for the entire set of L&P scenarios at once. The optimal solution should correspond to a trigeneration system containing the lowest equipment capacities able to efficiently operate in all L&P scenarios with minimal energy consumption. Accordingly, the decision variables of the problem are separated into

scenario-dependent and scenario independent variables. The latter group contains the design variables that are not affected by the uncertain parameters, which comprise all equipment sizing variables. Instead, the scenario-dependent variables are highly sensitive to the uncertain search space thereby providing a recourse against possible infeasibilities that could arise from a particular uncertainty materialization [21]. In this multiscenario framework, the operating decision variables (including heating, cooling and electricity generation; electricity purchased from and sold to the grid; part-load efficiencies; part-load performance features) are scenario-dependent optimization variables. In pursuit of the aforementioned goal of obtaining the most cost-effective design and operation of CHCP systems, we consider the minimization of the expected value for the total annualized cost distribution as the objective function. This objective function accounts for the capital investment in equipment and O&M expenditures (scenario independent decision variables) and operating expenses related to electricity and fuel consumption (scenario-dependent variables).

3. Methodology

3.1. Superstructure

As aforementioned, the modelling approach for the synthesis and optimization of CHCP systems is based on the general superstructure exhibited in **Fig. 1**. The superstructure embraces several thermal equipment pieces adequately integrated to generate electricity, heating and cooling. The equipment units are directly linked to a thermal energy storage unit to improve overall plant efficiency. Under such a system configuration, spark ignited ICEs fuelled by natural gas are used as prime movers for the simultaneous power and heat production into the cogeneration plant. Spark-ignition ICE configurations are well-established technologies widely applied in industrial facilities, as well as residential and

institutional/commercial buildings (*e.g.*, hospitals, hotels, water treatment facilities, to name a few) for meeting hot water requirements and/or space heating. Single or multiple ICE units –with capacities usually ranging from 10 kW to 18 MW– can be employed in cogeneration plants [22].

Whereas thermal and electrical load requirements are fulfilled by the ICE units, we consider a bidirectional grid connection to allow electricity purchase and sale for responding to any power shortage and excess, respectively. In addition, natural gas-fired boilers are utilized as auxiliary energy sources to meet energy demands. The main components of the trigeneration system also include the TES unit that is operated in charging and discharging modes for more efficient energy usage by decoupling thermal and power generation. The thermal energy from the TES tank can be either used to directly fulfil heating loads or cover cooling demands via ACH units. It should be noted that the employment of multiple equipment pieces with discrete sizes and rated capacities is allowed for the ICE, GFB and ACH technologies. For simplifying the mathematical formulation, we only consider the installation of equivalent units for each technology to restrict the number of different part-load performance curves (generally expressed by nonlinear and non-convex functions) required in the model.

3.2. Uncertainty characterization and scenarios generation

Fluctuations in energy load demands and energy prices may be significant over the CHCP systems lifetime (*e.g.*, 10–20 years). While accurate energy load estimations are difficult to forecast within the plant life-cycle period, the intrinsic uncertainty of energy prices can also have an important effect on the system energy and economic performances [8,23]. For better understanding of how long-term uncertainties can affect the cost-efficiency of CHCP systems, we treat all energy demands (including heating, cooling and electrical

loads) and energy prices (including natural gas price and electricity purchasing and selling tariffs) as uncertain (stochastic) design parameters. Additionally, we consider that uncertain price parameters can be correlated within a large-scale timeframe. To do so, we assume that all uncertain parameters can follow Normal (Gaussian) correlated (energy prices) and/or uncorrelated (energy loads) distributions. Note that multivariate Normal probability distributions are widely used in the literature to describe the uncertainty in energy loads and prices [8,16,20,23]. In this way, the uncertain parameters are mathematically modelled through multivariate Normal probability distributions as a set of representative L&P scenarios with known probability of occurrence. It should also be noted that the same probability of occurrence is presumed for all L&P scenarios. Hence, each L&P scenario expresses a unique combination of random values, or a sole sample, extracted from the Normal probability distributions for the uncertain load and price parameters. Thus, each L&P scenario describes a discrete value combination of uncorrelated energy load parameters (*i.e.*, heating, cooling and electricity demands) and correlated price parameters (*i.e.*, natural gas price and electricity purchasing and selling tariffs). Energy and economic random values limited by distributions boundaries are generated via a Monte Carlo sampling technique with symmetric correlation matrix. The Mersenne twister-based algorithm [24] for random values generation was implemented in MATLAB.

As fluctuating electricity and fuel prices, as well as their ratio (often referred to as spark spread), can greatly influence the long-term economic viability of CHCP systems [15,25,26], we assume that the uncertain energy prices can be correlated in this new stochastic approach. The probability density function for the correlated continuous random variables $X_1, X_2, ..., X_d$, where each one is expressed by a univariate (or marginal) Normal distribution can be defined as follows.

$$f_X\left(X_1, X_2, ..., X_d\right) = \left(\sqrt{\left(2\pi\right)^2 \left|\Sigma\right|}\right)^{-1} \cdot \exp\left(-0.5\left(X-\mu\right)^T \Sigma^{-1}\left(X-\mu\right)\right) \quad (1)$$

In **Eq. (1)**, μ denotes the d-dimensional vector of expected mean values (nominal) for each random variable (μ). Σ refers to the covariance matrix ($d \times d$), whilst $|\Sigma|$ is its determinant. Σ is a symmetric positive definite matrix wherein the diagonal elements contain the variances for each variable (σ_i^2), and the off-diagonal elements comprise the covariances between variables (σ_{ij}). It is noteworthy that a diagonal covariance matrix (*i.e.*, all covariances are null) indicates that there is no correlation between the random variables. Hence, the scenario generation framework requires the attribution of the covariance matrix in addition to the expected values and variances for the uncertain parameters. The off-diagonal elements in the covariance matrix can be obtained from the matrix of correlation ρ_{ij} given by,

$$\rho_{ij} = \sigma_{ij} / \sigma_i^2 \sigma_j^2 \quad (2)$$

Since the symmetric correlation matrix contains information about each pair of correlated random values, it can be used to describe the interactions between the uncertain parameters by setting all off-diagonal elements with values ranging from -1 to 1. In this particular case, we set positive correlations for energy prices by assuming typical trends of cross-energy European markets [27]. Correlated pricing scenarios obtained from this framework by considering a standard deviation of 20% from the expected mean values (0.04 US$ (kWh)$^{-1}$ for the natural gas price and 0.12 US$ (kWh)$^{-1}$ for the electricity purchasing tariff as retrieved from Ref. [28]) and distinct matrix correlation factors are depicted in **Fig. 2**. Although we only consider positive correlations for the uncertain

energy prices (here, the uncertain energy demands are generated as a set of uncorrelated stochastic parameters), the proposed methodology can be easily extended to account for positive and/or negative correlations between any pair (or even group) of random variables, without loss of generality of the proposed method. In addition, we consider Normal distributions for the sake of simplicity; however, this approach can also handle any kind of probability distribution. It is also noteworthy that the set of L&P scenarios generated from previous approach along with their related probabilities are used as input data to solve the stochastic multiscenario model (presented in next sections), which allows obtaining a distribution of results for each scenario-dependent variable.

Some final remarks should be made regarding the well-known concern in Stochastic Programming about the required number of scenarios to correctly solve the stochastic model. As expected, the model accuracy generally increases as a higher number of scenarios is considered during the optimization process. However, the size and complexity of the model and, consequently, the CPU time to find feasible solutions also increases due to the current algorithmic and computational limitations. Typically, the best number of scenarios is chosen by balancing the computational effort with the larger number of scenarios for which the difference between two consecutive sets does not present significant variations in terms of the optimal solutions found (an interested reader is addressed to Law and Kelton [29] for further details on this issue). Hence, additional attention should be paid to maintain the number of scenarios to a moderate level to ensure that the model can be solved with a reasonable computational cost [5].

3.3. Optimization strategy

Decision-making under uncertainty is a complex task, in which the decision maker needs the assistance of effective optimization approaches to deal with the wide range of possible alternatives. As deterministic approaches are not able to capture the dynamic behaviour of energy demands and prices, our modelling approach relies on a stochastic optimization strategy. For reducing the problem size and thereby the computational effort, stochastic model optimizations are performed by considering hourly-averaged load and price values for descriptive yearly periods (*i.e.*, representing important seasonal weather and prices variations) within the available timeframe dataset [30]. As the global optimal solution in this type of problem should always correspond to the sum of optima of each timestep –in which each optimal solution has no information about previous timesteps–, we consider a single optimization problem solved for an entire set of representative scenarios for the whole-time domain (see the case study) [8]. As mentioned before, the number of scenarios is chosen to be the smallest set which guarantees that the solutions found are completely stable and roughly coincident with those achievable when adopting the entire set of hourly timesteps (8760 h). In addition, the probabilistic scenarios are generated with standard deviations from expected mean values, which are consistent with the energy and price peaks measured within the whole-time domain to ensure system reliability. This optimization strategy ensures that optimal solutions can be found by using state-of-the-art MINLP solvers within reasonable computation times. In fact, the global optimum cannot be guaranteed if a metaheuristic-based approach is used to solve this problem. The mathematical formulation is developed as follows.

4. Stochastic multiscenario model

The mathematical model for the optimization of CHCP systems under uncertainty is developed via a multi-scenario MINLP-based formulation. An economic-oriented modelling approach is proposed for the cost-effective synthesis, design and operation, in which binary variables represent the discrete decisions about the selection and on/off status of each equipment unit at each L&P scenario. The simultaneous model encompasses electricity and thermal balances, demand and capacity constraints, equipment sizing equations and operating (off-design) performance curves, which should be considered to optimize the economic objective function. In the stochastic multiscenario approach, the model constraints should explicitly capture the effect of the uncertain parameters (including energy demands and prices) on the optimal CHCP system synthesis and operation. It is worth mentioning that the sizing-related decision variables are not affected by these uncertainty sources. For this reason, equipment capacities are defined as scenario independent decision variables. Conversely, all operating performance variables are scenario-dependent decision variables. Since both capital and operating expenses are considered for the cost-effective optimization of the CHCP system, the uncertain design parameters should also affect the objective function. In this work, we consider the minimization of the expected total annualized cost as the stochastic objective function. The following index sets are defined for better developing of the mathematical model.

$$I = \{ i / i \text{ is an equipment unit} \}$$

$$S = \{ s / s \text{ is a loading and pricing (L \& P) scenario} \}$$

For assessing the importance of adopting a stochastic programming approach rather than a conventional deterministic one, solutions obtained from the stochastic model should be compared with those from the deterministic approach. Observe that the deterministic model can be directly obtained from the proposed stochastic approach by setting a unique optimization scenario. Such a trending scenario is defined by the expected mean values for the energy loads and prices within the reference timeframe. The deterministic approach allows obtaining an optimal solution regarding the system configuration and operating conditions.

4.1. Electricity and thermal demand constraints

The energy demands should be met in all L&P optimization scenarios. For ensuring full coverage of electricity demands, the balance constraint **(3)** is considered.

$$\sum_{i\in I} E_{i,s}^{ICE} + E_s^{Purchase} - \left(E_s^{Sell} + \tilde{E}_s^{D}\right) = 0 \qquad \forall s \in S \tag{3}$$

The first term in **Eq. (3)** stands for the electric power generated by the cogeneration units in each L&P scenario $s \in S$, while $\tilde{E}_s^{D}$ indicates the uncertain parameter of electricity load demand in the $(s)th$ scenario. To deal with possible power shortages and surpluses, the decision variables $E_s^{Purchase}$ and E_s^{Sell} are used to allow the electricity purchasing from and selling to the grid, respectively. In each scenario, electricity can be either purchased from or sold to the grid (this is a plausible assumption, since the scenario s also corresponds to a different timestep as discussed before) [8]:

$$E_s^{Purchase} \cdot E_s^{Sell} = 0 \qquad \forall s \in S \tag{4}$$

Heating and cooling demand constraints are defined in **(5)** and **(6)**:

$$Q_{OUT_s}^{TES} - \sum_{i \in I} Q_{C_{i,s}}^{ACH} \geq \tilde{Q}_{H_s}^{D} \quad \forall s \in S \tag{5}$$

$$\sum_{i \in I} Q_{i,s}^{ACH} - \tilde{Q}_{C_s}^{D} = 0 \quad \forall s \in S \tag{6}$$

In inequality **(5)**, $Q_{OUT_s}^{TES}$ refers to the thermal power (in kW) obtained from the TES tank for meeting the energy requirements by the set of ACH units and the heating demand in each scenario $s \in S$. The variable $Q_{C_{i,s}}^{ACH}$ is defined as the amount of heat required by each ACH unit $i \in I$ for cooling production in each scenario s, whilst the variable $Q_{i,s}^{ACH}$ is the related power production (output) of each ACH unit needed to satisfy the cooling load demand. In addition, $\tilde{Q}_{H_s}^{D}$ and $\tilde{Q}_{C_s}^{D}$ are the uncertain parameters of heating and cooling demands, correspondingly. It is noteworthy that **(5)** is imposed as an inequality constraint to explore possible solutions in which the CHCP system does not strictly operate according to the FTL operating strategy. In this case, the surplus heat can be removed by exhausting hot gases. Since the production excess of cooling energy is not case profitable, the coverage of cooling load demands is imposed as the equality constraint shown in **Eq. (6)** [15].

The electricity production reliability index ($EPRI$) in **Eq. (7)** is used to restrict the search space, while ensuring the power production reliability of the cogeneration plant [31].

$$EPRI = \left(\sum_{s \in S} \tilde{E}_s^{D} - \sum_{i \in I} \sum_{s \in S} E_{i,s}^{ICE} \right) \Big/ \sum_{s \in S} \tilde{E}_s^{D} \tag{7}$$

A value of 0 for this index indicates that the system is able to account for all the electric power demand, whereas 1 specifies that the electricity loads are never met. For the optimal system design, constraint **(8)** should be satisfied:

$$EPRI \leq EPRI^{upper} \tag{8}$$

$EPRI^{upper}$ is the upper bound for the electricity production reliability index. Although this constraint is not strictly necessary, it generally produces improved economic performance solutions.

4.2. Operation priority constraints

As discussed before, the superstructure allows the use of multiple equipment pieces with discrete sizes and rated capacities for the ICE, GFB and ACH technologies. However, only equivalent units (*i.e.*, with the same part-load performance curves) are considered for each technology to simplify the mathematical formulation. For this reason, the equipment operation priority should be specified to avoid multiple equal solutions. For instance, if two ICE units are required in the cogeneration plant, the selection of the status "on" for the first engine and "off" for the second one in a given scenario would provide the same amount of electricity generated as if, instead, the status "off" is selected for the first unit and "on" for the second one [32]. The equipment functioning priority within the trigeneration system is given by the following constraints.

$$\left.\begin{aligned} E_{i,s}^{ICE} &\geq E_{i+1,s}^{ICE} \\ Q_{i,s}^{GFB} &\geq Q_{i+1,s}^{GFB} \\ Q_{i,s}^{ACH} &\geq Q_{i+1,s}^{ACH} \end{aligned}\right\} \forall i \in I,\ s \in S \tag{9}$$

These constraints define the operation order by ensuring that the $(i)th$ equipment unit is always selected before the $(i+1)th$ one. Therefore, they are required to reduce the search space and thereby the computational effort by eliminating irrelevant solutions.

4.3. Cogeneration plant: Internal Combustion Engines (ICEs)

Let $y_{i,s}^{ICE}$ be the binary variable that indicates the selection and on/off status of each ICE unit in the scenario s, in which,

$$y_{i,s}^{ICE} = \begin{cases} 1 & \textit{if the ICE unit i is used in the scenario s} \\ 0 & \textit{otherwise} \end{cases}$$
$$\forall i \in I,\ s \in S$$

The cogeneration operator in **(10)** is used to ensure the optimal selection and operation (on/off status) of the ICE unit $i \in I$ within the CHCP system in each scenario $s \in S$.

$$\begin{aligned}
&E_{i,s}^{ICE} = \eta_{Ei,s}^{ICE} \cdot F_{i,s}^{ICE} \qquad \forall i \in I,\ s \in S \\
&Q_{i,s}^{ICE} = \eta_{Qi,s}^{ICE} \cdot E_{i,s}^{ICE} \ \Big/ \eta_{Ei,s}^{ICE} \qquad \forall i \in I,\ s \in S \\
&\left.\begin{aligned} &\underline{E}_i^{ICE} \cdot y_{i,s}^{ICE} \le E_{i,s}^{ICE} \le \overline{E}_i^{ICE} \cdot y_{i,s}^{ICE} \\ &0 \le Q_{i,s}^{ICE} \le \overline{Q}^{ICE} \cdot y_{i,s}^{ICE} \end{aligned}\right\} \forall i \in I,\ s \in S \\
&E_{i,s}^{ICE} \ge 0,\ Q_{i,s}^{ICE} \ge 0,\ F_{i,s}^{ICE} \ge 0,\ y_{i,s}^{ICE} \in \{0,1\} \qquad \forall i \in I,\ s \in S
\end{aligned} \tag{10}$$

The decision variable $F_{i,s}^{ICE}$ indicates the fuel (natural gas) consumption by the cogeneration unit $i \in I$ in each scenario $s \in S$, while $Q_{i,s}^{ICE}$ is the corresponding thermal production. The electrical $\eta_{Ei,s}^{ICE} = f\left(\eta_{E,N}^{ICE}, LF_{i,s}^{ICE}\right)$ and thermal $\eta_{Qi,s}^{ICE} = f\left(\eta_{Q,N}^{ICE}, LF_{i,s}^{ICE}\right)$

efficiencies of the unit $i \in I$ in each scenario $s \in S$ are obtained from the part-load performance curves for ICEs presented in **Table 1**. Additionally, $\underline{E}_i^{ICE}$ and $\overline{E}_i^{ICE}$ refer to the lower and upper bounds for the electric power production $E_{i,s}^{ICE}$, respectively. Note that the electricity generation of each engine should be limited between 50 – 100% of the corresponding nominal power capacity. In this work, the nominal capacity of each prime mover unit $i \in I$ (W_i^{ICE}) lies in the range of 600 to 1600 kW (in 11 different discrete power intervals of 100 kW). Thus, the power capacity selection is given by **(11)**.

$$\left.\begin{aligned} & W_i^{ICE} = 600 \cdot y_{i,1}^{ICE,N} + 700 \cdot y_{i,2}^{ICE,N} + \ldots + 1600 \cdot y_{i,11}^{ICE,N} \\ & \sum_{n=1}^{11} y_{i,n}^{ICE,N} = 1 \end{aligned}\right\} \forall i \in I \tag{11}$$

Similar energy operators are used for modelling the optimal selection and operation (on/off status) of auxiliary GFB and ACH units, which are presented as follows.

4.4. Heat production: Gas-fired boilers (GFBs)

Let $y_{i,s}^{GFB}$ be the binary variable that indicates the selection and on/off status of each GFB in the scenario $s \in S$. Thus, formulation **(12)** is used to model the optimal operation of GFB units in the CHCP system for each scenario $s \in S$.

$$\begin{aligned} & Q_{i,s}^{GFB} = \eta_{i,s}^{GFB} \cdot F_{i,s}^{GFB} \quad \forall i \in I, s \in S \\ & 0 \le Q_{i,s}^{GFB} \le \overline{Q}^{GFB} \cdot y_{i,s}^{GFB} \quad \forall i \in I,\ s \in S \\ & Q_{i,s}^{GFB} \ge 0,\ \eta_{i,s}^{GFB} \ge 0,\ F_{i,s}^{GFB} \ge 0,\ y_{i,s}^{GFB} \in \{0,1\} \quad \forall i \in I,\ s \in S \end{aligned} \tag{12}$$

$Q_{i,s}^{GFB}$ represents the thermal power production that is expressed as a function of the natural gas consumption $F_{i,s}^{GFB}$ of the GFB unit $i \in I$ in each scenario $s \in S$. The GFB efficiency $\eta_{i,s}^{GFH} = F\left(\eta_N^{GFB}, LF_{i,s}^{GFB}\right)$ is given by the part-load performance curve presented in **Table 1**. In addition, the parameter $\overline{Q}^{GFB}$ is the upper bound for the thermal production, which corresponds to the rated capacity ($Q_R{}^{GFB}$) of the auxiliary boilers (see **Table 2**).

4.5. Cooling production: Absorption chillers (ACHs)

The typical part-load energy performance of a single-effect ACH is given as follows [1,33].

$$\begin{aligned}
&COP_{i,s}^{ACH} = COP_R^{ACH} \cdot \left(Qc_{i,s}^{ACH} / Q_R^{ACH}\right) / C_{LF\,i,s} \qquad \forall i \in I,\ s \in S \\
&0 \le Q_{i,s}^{ACH} \le \overline{Q}^{ACH} \cdot y_{i,s}^{ACH} \qquad \forall i \in I,\ s \in S \\
&COP_{i,s}^{ACH} \ge 0,\ Qc_{i,s}^{ACH} \ge 0,\ Q_{i,s}^{ACH} \ge 0,\ y_{i,s}^{ACH} \in \{0,1\} \qquad \forall i \in I,\ s \in S
\end{aligned} \tag{13}$$

$COP_{i,s}^{ACH}$ is the coefficient of performance of the ACH unit $i \in I$ in each scenario $s \in S$. The thermal consumption $Qc_{i,s}^{ACH}$ of each ACH unit is obtained as in **Eq. (14)**.

$$Qc_{i,s}^{ACH} = C_{LF\,i,s} \cdot C_{\overline{T}} \cdot Q_R^{ACH} \qquad \forall i \in I,\ s \in S \tag{14}$$

In **Eq. (14)**, $C_{LF\,i,s}$ and $C_{\overline{T}}$ refer to the correction coefficients for the load rate and cooling water temperature, respectively, as shown in **Table 1**.

4.6. Thermal energy storage (TES)

The amount of thermal energy stored in the TES tank at each L&P scenario s is given by **Eq. (15)** [31,34].

$$\begin{aligned} Q_s^{TES} &= \left(Q_{IN_s}^{TES} - Q_{OUT_s}^{TES}\right)\Big/\eta^{TES} \qquad \forall s = 1 \\ Q_s^{TES} &= Q_{s-1}^{TES}\cdot\left(1-\varepsilon\right) - \left(Q_{OUT_s}^{TES} - Q_{IN_s}^{TES}\right)\Big/\eta^{TES} \qquad \forall s > 1 \end{aligned} \tag{15}$$

In which,

$$Q_{IN_s}^{TES} = \sum_{i\in I} Q_{i,s}^{ICE} + \sum_{i\in I} Q_{i,s}^{GFB} \qquad \forall s \in S \tag{16}$$

In **Eq. (15)**, ε represents the energy loss coefficient that depends on the thermal insulation of the TES tank. Moreover, η^{TES} is the thermal storage efficiency. The capacity of the TES tank is determined by constraint **(17)**:

$$C^{TES} \geq Q_s^{TES} \qquad \forall s \in S \tag{17}$$

4.7. Stochastic objective function

The resulting stochastic multiscenario MINLP-based model is optimized through the minimization of the expected value of the total annualized cost distribution (TAC^{Exp}). The stochastic objective function can be formally expressed as follows:

$$\begin{aligned} \min \quad & TAC^{Exp} = \sum_{s=1}^{S} prob_s \cdot TAC_s \\ s.t. \quad & Eq.(3) - (17) \end{aligned} \tag{18}$$

The parameter $prob_s$ stands for the probability of occurrence of a specific optimization scenario s. We consider the same probability of occurrence for all L&P scenarios. The decision variable TAC_s represents the total annualized cost distribution of the trigeneration system over the different optimization scenarios, which is composed by the capital investment in equipment ($CAPEX$) and operating expenditures ($OPEX_s$) as stated by **Eq. (19)**.

$$TAC_s = CAPEX + OPEX_s \qquad \forall s \in S \tag{19}$$

In which,

$$CAPEX = f_{ac} \cdot \left[\begin{array}{l} \left(\frac{CEPCI^{2017}}{CEPCI^{2013}} \right) \cdot F_{BM}{}^{ICE} \cdot \sum_{i \in I} C_{PO_i}^{ICE} + \left(\frac{CEPCI^{2017}}{CEPCI^{2003}} \right) \cdot F_{BM}{}^{GFB} \cdot \sum_{i \in I} C_{PO_i}^{GFB} + \\ F_{BM}{}^{ACH} \cdot \sum_{i \in I} C_{PO_i}^{ACH} + F_{BM}{}^{TES} \cdot \sum_{i \in I} C_{PO_i}^{TES} \end{array} \right] \tag{19a}$$

$$OPEX_s = \left[\begin{array}{l} \left[\tilde{C}_s^{NG} \cdot \left(F_s^{ICE} + F_s^{GFB} \right) \right]^{Fuel} + \left[\tilde{C}_s^{Ptariff} \cdot E_s^{Purchase} - C^{Stariff} \cdot E_s^{Sell} \right]^{Electricity} + \\ \left[C_{O\&M}^{ICE} + C_{O\&M}^{GFB} + C_{O\&M}^{ACH} + C_{O\&M}^{TES} \right]^{Operating\ \&\ Maintenance\ expenses} \end{array} \right] \qquad \forall s \in S \tag{19b}$$

Since the capacity of the acquired equipment units must remain unchanged for all L&P scenarios, the related capital investment should be defined by a scenario independent decision variable. Conversely, the operating expenses should be given by a scenario-dependent variable to capture the energy consumption variability and ensure system flexibility in the uncertain optimization search space. In **Eq. (19a)**, C_{PO} represents the unitary cost of equipment (in kUS$) running at near ambient-pressure conditions, while F_{BM} indicates the cost correction factor based on operating conditions and construction

materials. In this work, we use the nominal capacity-based cost correlations obtained from Urbanucci and Testi [8] for the cogeneration units (ICEs), Couper et al. [35] for the GFB units, and Lorestani and Ardehali [31] for the ACH and TES units, to estimate the capital investment of each equipment piece required into the trigeneration system. It should be noted that the capital cost correlations are updated for the reference year (2017) through the Chemical Engineering Plant Cost Index (CEPCI) [36]. The CEPCI ratios, as shown in **Eq. (19a)**, are the relative cost index for equipment of the reference year (2017) to the year in which the cost correlations were originally presented in literature. Thus, they allow to convert the capital costs to the equivalent values in 2017. In this case, the CEPCI index ratios for ACH's and TES's cost correlations are both considered to be equal to 1. In addition, the annualization factor for the capital investment fac is obtained as in **Eq. (20)** [37]:

$$fac = ir \cdot (1+ir)^{t} \cdot \left[(1+ir)^{t} - 1 \right]^{-1} \tag{20}$$

In which ir defines the fractional interest rate per year during the amortization period t. In **Eq. (19b)**, $\tilde{C}_s^{NG}$ and $\tilde{C}_s^{Ptariff}$ are the uncertain parameters for the cost of natural gas and electricity purchasing tariff, respectively, in each L&P scenario obtained through the proposed stochastic approach. Moreover, the parameter $C^{Stariff}$ refers to the electricity selling tariff to the grid, while the variable $C_{O\&M}$ represents the operating and maintenance expenditures of each equipment.

The resulting multiscenario MINLP model was implemented in GAMS (version 24.9.2) [38] and solved to global optimality via the deterministic global branch-and-bound solver ANTIGONE (Algorithms for coNTinuous/Integer Global Optimization of

Nonlinear Equations), with the sub-solvers SNOPT and CPLEX 12.7. A computer with an Intel® Core™ i5-3570 M 3.4 GHz processor and 8 GB RAM running Windows 10 was used to solve the case study.

5. Case Study

An illustrative case study is carried out to evaluate the capabilities of the proposed stochastic approach for the optimal synthesis, design and operation of CHCP systems under uncertainty in energy loads and prices. **Fig. 1** depicts the superstructure considered for the optimal CHCP system design with thermal energy storage and bidirectional electricity grid connection. **Table 2** shows the nominal efficiencies and rated capacities of the different technologies used for electricity, heating, and cooling generation, as well as thermal storage in the trigeneration system. For stochastic optimizations, the natural gas price and electricity purchasing tariff are uncertain correlated parameters generated via the aforementioned sampling technique as depicted in **Fig. 2**. Conversely, the electricity selling tariff is treated as a known design parameter (deterministic). Thermal energy storage with no energy losses is assumed in the CHCP system. The relative cooling water temperatures are obtained from Ref. [1]. Additionally, an electricity production reliability index of $EPRI \leq 0.002$ is considered for all problem optimizations.

The multiscenario MINLP-based model can be used for different industrial, residential, commercial and services applications including single and multiple buildings, such as hospitals, hotels, schools, universities, among others. In this work, the case study is based on the energy consumption information from a typical hotel and spa facility located at the northern region of Portugal. The hotel works on a 24-hour timetable in a building area of ~20,000 m^2, encompassing nearly 300 guest rooms and suites, conference rooms, heated indoor pool, sauna, beauty salon, lounge restaurant and bar, and laundry

services. As mentioned before, we adopt an optimization strategy based on hourly-averaged load and price values obtained from descriptive yearly periods within the available timeframe dataset to reduce the problem size and thereby the computational effort. In this case study, the consumption data for cooling, heating and electricity loads have been obtained from 3 representative weeks in summer, winter and transitional seasons [8]. The long-term uncertainty of energy demands and prices is described by a set of correlated L&P scenarios generated using the proposed Monte Carlo-based sampling technique. To do so, we assume Normal distributions with 20% of relative standard deviation from the expected mean values for each uncertain parameter. This value is consistent with the 6-consecutive-year data obtained for energy demands and prices in the hotel facility reference case. **Fig. 3** exhibits the load duration curves of the electricity, heating and cooling demands obtained for the case study. Additionally, uncertain natural gas costs and electricity tariffs are correlated through a matrix factor (or degree of correlation) of +0.8, which is also in accordance with the longstanding energy prices correlation detected in the cross-energy European markets [27]. Expected mean values for the natural gas price and electricity purchasing tariff, in addition to other economic evaluation data, are presented in **Table 3**.

6. Results and Discussion

6.1. Deterministic vs stochastic results

Firstly, we solve the deterministic model through the minimization of the total annualized cost. It should be noted that, in this case, the entire set of energy demands (*i.e.*, heating, cooling and electricity loads) and energy prices (*i.e.*, natural gas and electricity purchasing and selling tariffs) are known deterministic parameters corresponding to the expected mean values. These parameters are used as input data for solving the deterministic model.

The optimal configuration obtained for the CHCP system is composed by an ICE unit with nominal power capacity of 1300 kW ($\eta_E^{ICE} = 0.37$; $\eta_Q^{ICE} = 0.33$), as well as an auxiliary boiler (with rated capacity of 960 kW and thermal production of 933.6 kW) and an ACH unit (with rated capacity of 1300 kW and thermal production of 750 kW) required to meet heating and cooling loads, respectively. The cogeneration unit is able to account for all the electrical demand so that no electricity is either purchased or sold to the grid. No energy storage is needed in the system. The total annualized cost for the optimal deterministic solution is equal to 2109 kUS$ year^{-1}, which is comprised by 486 kUS$ year^{-1} related to the capital investment and 1623 kUS$ year^{-1} associated with operating expenditures (maintenance and fuel consumption).

Henceforth, the design and optimization of CHCP systems is performed via the proposed stochastic multiscenario model. In the stochastic solution, the optimal system configuration encompasses a cogeneration plant with power capacity of 1400 kW, in addition to an auxiliary boiler (960 kW) and an ACH unit (1300 kW). The increase in the ICE unit capacity indicates an adjustment of the system to ensure the optimal operating performance in all different scenarios. The system also requires a storage tank with capacity for 2862.13 kW of thermal energy. The expected total annualized cost for the optimal stochastic solution is 2243 kUS$ year^{-1}, from which 526 kUS$ year^{-1} is related to the capital investment. **Fig. 4** depicts the distribution of the total annualized cost of the CHCP system obtained through the minimization of the stochastic objective function.

In the solution under examination, the expected total annualized cost and capital investment are, respectively, ~6% and 8% higher than the corresponding deterministic optimal solutions. These differences suggest that the total costs of the trigeneration system may be underestimated by the conventional deterministic method. Moreover, if the equipment capacities obtained via the deterministic model are fixed when solving the

stochastic one, the problem becomes infeasible and optimal solutions cannot be found by the stochastic approach. This result clearly indicates that the optimal deterministic solution provides neither the flexibility nor the cost-effectiveness required by the CHCP system to operate under fluctuating demand and price conditions.

As concerns the operational expenses, the distribution obtained via the stochastic approach shows that ~42% of the L&P scenarios present values higher than the equivalent deterministic solution. **Fig. 5** displays the operating expenses distribution throughout the different L&P scenarios, where the first 48 scenarios are zoomed in to show the different components of the referred cost. In **Fig. 5**, scenario 2, for example, exhibits operating expenses equal to 2626 kUS$ year^{-1}, which is a value nearly 62% greater than that estimated by the deterministic model. In such a scenario, 2232 kUS$ year^{-1} are related to fuel consumption by the ICE and GFB units, while the electricity expenses accounts for 351 kUS$ year^{-1}. Note that the remaining costs are related to maintenance expenditures. However, the distribution in the uncertain search space reveals even higher values for operating expenses. For instance, the scenario 163 presents operating costs of 3146 kUS$ year^{-1}, which is ~94% higher than the deterministic value.

While no energy storage tank is required in the deterministic solution, the stochastic approach provides a thermal storage distribution throughout the L&P scenarios as shown in **Fig. 6**. Similar distributions over the different scenarios are obtained for each scenario-dependent decision variable, including the fuel consumption by the ICE and GFB units, electricity and thermal generation by the ICE unit, electricity purchase and selling and cooling production by the ACH unit, to list a few. Some profiles for energy production and consumption are examined in the next section, whilst the remaining distributions are not presented here for the sake of brevity. Regardless of the results distribution analysed, all energy consumption and production profiles obtained highlight

the significant influence of load and price uncertainties on the optimal operating performance of CHCP systems. Since the deterministic model is not able to provide energy and economic performance distributions, our results strongly emphasize the importance of adopting a stochastic approach to deliver robust solutions and capture the effects of different types of uncertainty.

6.2. Stochastic CHCP system optimization and risk analysis

For an improved understanding of the broad impact of the uncertainty on the optimal CHCP system design and operation, more articulate analysis is required concerning the results obtained through the stochastic approach. **Fig. 7 (*a*)** illustrates the electric power profiles for the electricity generated by the ICE unit, as well as the electricity purchased from and sold to the grid and energy demands in 72 distinct scenarios. **Fig. 7 (*b*)** shows the related profiles for the electricity purchasing tariffs and natural gas prices. **Fig. 8** displays the thermal power profiles for the heating production by the ICE and GFB units, and the heating demands in the same 72 distinct scenarios. A thorough examination of **Fig. 7** reveals that the CHCP system prioritizes the electricity production by the ICE unit over its acquisition from the grid. This is an expected result since the natural gas prices are, in general, much lower than the electricity tariffs in all scenarios. Overall, the electricity purchasing occurs in two main situations: (*i*) the scenarios present high energy demands –*i.e.*, higher than the available capacity of the ICE unit–, even if the energy prices are high (*e.g.*, scenario 2, 18 and 36)–; and, (*ii*) the scenarios present a purchasing tariff more competitive than the natural gas price (scenario 5), even if the demands are low (scenario 34). In any case, the energy profiles clearly show that the correlated energy prices considerably affect the optimal CHCP system performance.

The financial risk associated with the uncertain search space is assessed by considering different standard deviations from the expected mean values of uncertain energy loads and prices, as well as distinct correlation degrees for energy prices. **Fig. 9** and **Fig. 10** display the cumulative probability curves obtained for the optimal economic performance of the CHCP system under low-correlation (+0.1) and high-correlation (+0.8) matrix factors, respectively. In both cases, standard deviations of 10%, 20% and 30% are considered to generate the L&P scenarios. To construct the probability curves, the scenarios are sorted in ascending order of their economic performance values. In those figures, the vertical axis shows the probability of reaching an economic performance (expressed by the total annualized cost) lesser than or equal to a target limit indicated in the horizontal axis. To illustrate this, let us assume a target value of 2598 kUS$ year^{-1} (upper bound for the 10%-curve) for the system total annualized cost. Thus, **Fig. 9** indicates that the 20% and 30% standard deviation curves have, respectively, ~6% and ~24% of probability of exceeding the referred economic target. Note that the 10%-curve has no probability of exceeding this value. If the decision-maker targets a more ambitious goal of 2300 kUS$ year^{-1}, for instance, then the probabilities of exceeding this limit are significantly increased to ~40% (10%-curve), ~46% (20%-curve) and ~62% (30%-curve).

When assuming higher correlation degrees between energy prices as shown in **Fig. 10**, the probabilities of exceeding the objective of 2300 kUS$ year^{-1} are slightly decreased to ~39% (10%-curve), ~42% (20%-curve) and ~58% (30%-curve). Nevertheless, these probabilities can increase as the correlation degree becomes higher when considering other target limits. This is the case of the target value of 2500 kUS$ year^{-1}, for which the exceeding probabilities are increased from 3% (10%-curve), 15% (20%-curve) and 34% (20%-curve), to 4% (10%-curve), 20% (20%-curve) and 36%

(20%-curve). The probabilities of exceeding the maximum value obtained for the total annualized cost in the 10%-curve (*i.e.*, 2791 kUS$ year^{-1}) are equal to ~8% and ~18% for the 20%-curve and 30%-curve, correspondingly.

Regardless of the correlation degree, these results indicate that the probability of exceeding a prespecified value escalates as the standard deviation increases. Consequently, a closer inspection of **Fig. 9** and **Fig. 10** reveals that the assumption of higher standard deviations for uncertain design parameters implies a riskier decision-making attitude. Therefore, if the decision-maker selects the system design defined by the 10%-curve in **Fig. 9**, it is ensured that the total annualized cost will not surpass the maximum value of 2598 kUS$ year^{-1}. However, this conservative attitude would lead to the selection of a system design with an impaired overall economic performance. In this case, ~11% of the scenarios in the 30%-curve, for instance, exhibit a total annualized cost smaller than the lower limit of 1739 kUS$ year^{-1} obtained for the 10%-curve. Similar conclusions can be drawn from the examination of the curves in **Fig. 10**.

Due to the above-mentioned variations in the probabilities of exceeding specific targets, the decision-making process according to the correlation degree is not straightforward in this case study. Though, the general trend of the curves in both figures suggests that the selection of curves with higher correlation degrees (allied to higher standard deviations) also involves a riskier decision-making attitude. This result is supported by the significant differences found between the extreme solutions (lower and upper bounds for the total annualized cost) of the economic performance profiles under low and high correlation degrees. We report that the 20%-curve for the high-correlation degree (**Fig. 10**) presents lower and upper bounds around, respectively, 9% and 16% higher than the corresponding extreme values in the 20%-curve for the low-correlation degree (**Fig. 9**). This is due to the correlated parameters assuming the lowest (in the lower

bound) and highest (in the upper bound) values for both electricity and fuel prices in the uncertain search space, leading to extreme pricing scenarios. Still in **Fig. 9**, we report expected total annualized costs equal to 2221 kUS$ year^{-1} (20%-curve) and 2339 kUS$ year^{-1} (30%-curve). The corresponding values in **Fig. 10** are 2243 kUS$ year^{-1} (20%-curve) and 2361 kUS$ year^{-1} (30%-curve). Hence, besides the greater variability observed in the total annualized cost distribution for the same level of uncertainty, the expected costs also increase as higher correlation degrees are considered between the uncertain energy prices. These results demonstrate that energy prices correlations should also be taken into consideration during the decision-making process to properly evaluate all the effects of the uncertainty on the CHCP system performance. Finally, we report that additional risk metrics such as downside risk and worst case for the total annualized cost have been applied to solve this problem. However, the solutions found by the multi-objective optimizations have not shown significant trade-offs between the optimal Pareto alternatives.

7. Conclusions

Optimal synthesis, design and operation of trigeneration systems represent a major challenge, particularly considering that economic viability and financial risks are influenced by long-term uncertainties. For surpassing such difficulties, a novel stochastic model for the optimization of CHCP systems under uncertainty in energy loads and prices is introduced in this work. Our new economic-oriented approach relies on a stochastic multiscenario MINLP model aimed at enhancing system cost-effectiveness, while accounting for wide-ranging scenarios of energy demands and prices. For this purpose, a set of different probabilistic scenarios of energy loads (heating, cooling and electricity) and correlated energy prices (electricity and natural gas) are generated via Monte Carlo

sampling technique with a given probability of occurrence. Our optimization model is based on a general superstructure including energy production equipment, thermal storage and bidirectional grid connection. Energy operators are proposed to guarantee the optimal equipment selection and operation in each loading and pricing scenario. The resulting model was implemented in GAMS and solved to global optimality through the minimization of the expected total annualized cost. We evaluate the capabilities of the proposed new approach through an illustrative case study with reference to a Portuguese hotel facility.

To the best of our knowledge, this is the first stochastic multiscenario MINLP-based model for the optimization of CHCP systems to simultaneously address the energy demands uncertainty and the correlation between uncertain energy prices. Major contributions from this work can be summarized as follows:

- The new multiscenario modelling approach allows obtaining the most cost-effective CHCP design able to operate under long-term fluctuating energy demands and prices.
- The improved MINLP-based formulation ensures the optimal selection and operation (on/off status) of each equipment in the different scenarios.
- The stochastic modelling approach effectively handles the most important uncertainty factors all together, and also the correlation between several uncertain design parameters.
- The optimization strategy allied to the robust model formulation allows efficiently optimizing the problem to global optimality unlike preceding literature, which provides enhanced energy-efficiency solutions and computational performance.

- The systematic tool can be used for optimizing a variety of applications such as buildings within the residential and commercial sectors, or even in the industry.
- Robust stochastic solutions provide valuable new insights about the uncertainty effects on the CHCP system under evaluation, leading to an improved decision-making process.

Concerning the main results, some important points should be underlined:

- Our results emphasize the importance of using the stochastic approach over a conventional deterministic one to avoid underestimating process costs, and provide all flexibility and cost-effectiveness needed by CHCP systems to operate under varying loads and prices.
- Energy and economic performance distributions unequivocally indicate that the load and price uncertainties considerably affect the optimal design and operation of CHCP systems.
- Economic risks analysis reveals riskier decision-making as higher uncertainty levels are considered for uncertain design parameters.
- Numerical results also highlight the relevance of the correlation between energy prices in the assessment of the uncertainty effects on the CHCP system performance.

For the above-mentioned reasons, our systematic approach constitutes a useful tool to support decision-makers and planners towards the implementation of more robust and cost-effective CHCP systems. Future research will focus on the application of more complex probability distributions for each uncertain parameter, as well as studying further potential correlations between uncertain parameters (*e.g.*, thermal and electricity demands patterns, purchase and sell prices, energy demands and costs, *etc.*) and their impact on the optimal system performance. Additionally, the model extension may introduce

multicriteria decision analysis techniques for evaluating the trade-offs between conflicting goals including energy and environmental indicators.

Acknowledgements

This work was partially supported by projects UID/MULTI/00308/2019 and by the European Regional Development Fund through the COMPETE 2020 Programme, FCT – Portuguese Foundation for Science and Technology and Regional Operational Program of the Center Region (CENTRO2020) within the projects SUSpENsE (CENTRO-01-0145-FEDER-000006) and MAnAGER (POCI-01-0145-FEDER-028040).

Nomenclature

Acronyms

ACH	Absorption Chiller
CEPCI	Chemical Engineering Plant Cost Index
CHP	Combined Heating and Power
CHCP	Combined Heating, Cooling and Power
FEL	Following the Electric Load
FTL	Following the Thermal Load
GA	Genetic Algorithm
GAMS	General Algebraic Modeling System
GFB	Gas-Fired Boiler
ICE	Internal Combustion Engine
L&P	Loading and Pricing
MINLP	Mixed-Integer Nonlinear Programming
O&M	Operating and Maintenance
PSO	Particle Swarm Optimization
TES	Thermal Energy Storage

Greek letters

ε	Energy loss coefficient
η	Efficiency
η_E	Electrical efficiency
η_N	Nominal efficiency
η_Q	Thermal efficiency

m	Vector of expected nominal values
r	Matrix of correlation
å	Covariance matrix
s	Covariance

Roman letters

$\tilde{C}^{NG}$	Natural gas cost, US$ (kWh)$^{-1}$
$\tilde{C}^{Ptariff}$	Electricity purchasing tariff, US$ (kWh)$^{-1}$
$C^{Stariff}$	Electricity selling tariff, US$ (kWh)$^{-1}$
C^{TES}	Thermal capacity storage, kW
$CAPEX$	Capital cost of investment, kUS$ year^{-1}
C_{LF}	Correction coefficient for the load rate
$C_{O\&M}$	Operating and maintenance expenditures
COP	Coefficient of performance
COP_R	Rated performance coefficient
C_{PO}	Unitary cost of equipment, kUS$
$C_{\bar{T}}$	Correction coefficient for the cooling water temperature
E	Electric power, kW
$\tilde{E}^{D}$	Electricity demand, kW
$E^{Purchase}$	Electricity purchasing from the grid, kW
E^{Sell}	Electricity selling to the grid, kW
$EPRI$	Electricity production reliability index
F	Natural gas consumption, kW

f_{ac}	Annualization factor for capital cost
F_{BM}	Correction factor for capital cost
ir	Fractional interest rate per year
LF	Partial load factor
$OPEX$	Operational expenses, kUS$ year^{-1}
$prob$	Probability
Q	Thermal power, kW
$\tilde{Q}_C{}^D$	Cooling demand, kW
$\tilde{Q}_H{}^D$	Heating demand, kW
Q_R	Rated thermal capacity, kW
$\overline{T}$	Relative cooling water inlet temperature, K
t	Amortization period, years
TAC	Total annualized cost, kUS$ year^{-1}
TAC^{Exp}	Expected total annualized cost, kUS$ year^{-1}
X	Correlated continuous random variable
W	Nominal power capacity, kW
y	Binary variable that takes the value «1» if a given equipment is selected

Subscripts

i	Equipment unit
s	Scenario

References

[1] Wang X, Yang C, Huang M, Ma X. Off-design performances of gas turbine-based CCHP combined with solar and compressed air energy storage with organic Rankine cycle. Energy Convers Manag 2018;156:626–38. doi:10.1016/j.enconman.2017.11.082.

[2] Angrisani G, Akisawa A, Marrasso E, Roselli C, Sasso M. Performance assessment of cogeneration and trigeneration systems for small scale applications. Energy Convers Manag 2016;125:194–208. doi:10.1016/j.enconman.2016.03.092.

[3] European Parliament. Directive 2012/27/EU of the European Parliament and of the Council of 25 October 2012 on energy efficiency. Off J Eur Union Dir 2012:1–56. doi:10.3000/19770677.L_2012.315.eng.

[4] Al Moussawi H, Fardoun F, Louahlia-Gualous H. Review of tri-generation technologies: Design evaluation, optimization, decision-making, and selection approach. Energy Convers Manag 2016;120:157–96. doi:10.1016/j.enconman.2016.04.085.

[5] Mavromatidis G, Orehounig K, Carmeliet J. Design of distributed energy systems under uncertainty: A two-stage stochastic programming approach. Appl Energy 2018;222:932–50. doi:10.1016/j.apenergy.2018.04.019.

[6] Cho H, Smith AD, Mago P. Combined cooling, heating and power: A review of performance improvement and optimization. Appl Energy 2014;136:168–85. doi:10.1016/j.apenergy.2014.08.107.

[7] Wouters C, Fraga ES, James AM. Residential Microgrid Design Optimisation under Uncertain μCHP Characteristics. Comput Aided Chem Eng 2016;38:1491–6. doi:10.1016/B978-0-444-63428-3.50253-8.

[8] Urbanucci L, Testi D. Optimal integrated sizing and operation of a CHP system

with Monte Carlo risk analysis for long-term uncertainty in energy demands. Energy Convers Manag 2018;157:307–16. doi:10.1016/j.enconman.2017.12.008.

[9] Akbari K, Nasiri MM, Jolai F, Ghaderi SF. Optimal investment and unit sizing of distributed energy systems under uncertainty: A robust optimization approach. Energy Build 2014;85:275–86. doi:10.1016/j.enbuild.2014.09.009.

[10] Noussan M, Jarre M, Roberto R, Russolillo D. Combined vs separate heat and power production – Primary energy comparison in high renewable share contexts. Appl Energy 2018;213:1–10. doi:10.1016/j.apenergy.2018.01.026.

[11] Hossein Abbasi M, Sayyaadi H, Tahmasbzadebaie M. A methodology to obtain the foremost type and optimal size of the prime mover of a CCHP system for a large-scale residential application. Appl Therm Eng 2018;135:389–405. doi:10.1016/j.applthermaleng.2018.02.062.

[12] Ünal AN, Ersöz İ, Kayakutlu G. Operational optimization in simple tri-generation systems. Appl Therm Eng 2016;107:175–83. doi:10.1016/j.applthermaleng.2016.06.059.

[13] Wang Y, Shi Y, Luo Y, Cai N, Wang Y. Dynamic analysis of a micro CHP system based on flame fuel cells. Energy Convers Manag 2018;163:268–77. doi:10.1016/j.enconman.2018.02.064.

[14] Jiménez-Navarro JP, Kavvadias KC, Quoilin S, Zucker A. The joint effect of centralised cogeneration plants and thermal storage on the efficiency and cost of the power system. Energy 2018;149:535–49. doi:10.1016/j.energy.2018.02.025.

[15] Piacentino A, Gallea R, Catrini P, Cardona F, Panno D. On the Reliability of Optimization Results for Trigeneration Systems in Buildings, in the Presence of Price Uncertainties and Erroneous Load Estimation. Energies 2016;9:1049. doi:10.3390/en9121049.

[16] Gamou S, Yokoyama R, Ito K. Optimal unit sizing of cogeneration systems in consideration of uncertain energy demands as continuous random variables. Energy Convers Manag 2002;43:1349–61. doi:10.1016/S0196-8904(02)00020-1.

[17] Li C-Z, Shi Y-M, Liu S, Zheng Z, Liu Y. Uncertain programming of building cooling heating and power (BCHP) system based on Monte-Carlo method. Energy Build 2010;42:1369–75. doi:10.1016/j.enbuild.2010.03.005.

[18] Hu M, Cho H. A probability constrained multi-objective optimization model for CCHP system operation decision support. Appl Energy 2014;116:230–42. doi:10.1016/j.apenergy.2013.11.065.

[19] Wang L, Singh C. Stochastic combined heat and power dispatch based on multi-objective particle swarm optimization. Int J Electr Power Energy Syst 2008;30:226–34. doi:10.1016/j.ijepes.2007.08.002.

[20] Ersoz I, Colak U. Combined cooling, heat and power planning under uncertainty. Energy 2016;109:1016–25. doi:10.1016/j.energy.2016.04.071.

[21] Sahinidis N V. Optimization under uncertainty: state-of-the-art and opportunities. Comput Chem Eng 2004;28:971–83. doi:10.1016/j.compchemeng.2003.09.017.

[22] US Environmental Protection Agency. Catalog of CHP technologies. Combined Heat and Power Partnership 2017.

[23] Carpaneto E, Chicco G, Mancarella P, Russo A. Cogeneration planning under uncertainty. Appl Energy 2011;88:1059–67. doi:10.1016/j.apenergy.2010.10.014.

[24] Matsumoto M, Nishimura T. Mersenne twister: a 623-dimensionally equidistributed uniform pseudo-random number generator. ACM Trans Model Comput Simul 1998;8:3–30. doi:10.1145/272991.272995.

[25] Smith AD, Fumo N, Mago PJ. Spark spread - A screening parameter for combined heating and power systems. Appl Energy 2011;88:1494–9.

doi:10.1016/j.apenergy.2010.11.004.

[26] Kavvadias KC. Energy price spread as a driving force for combined generation investments: A view on Europe. Energy 2016;115:1632–9. doi:10.1016/j.energy.2016.03.058.

[27] Frydenberg S, Onochie JI, Westgaard S, Midtsund N, Ueland H. Long-term relationships between electricity and oil, gas and coal future prices-evidence from Nordic countries, Continental Europe and the United Kingdom. OPEC Energy Rev 2014;38:216–42. doi:10.1111/opec.12025.

[28] European Commission. Eurostat 2016.

[29] Law ML, Kelton WD. Simulation, Modeling and Analysis, 3rd ed. New York: McGraw Hill, 2000.

[30] Amusat OO, Shearing PR, Fraga ES. Optimal design of hybrid energy systems incorporating stochastic renewable resources fluctuations. J Energy Storage 2018;15:379–99. doi:10.1016/j.est.2017.12.003.

[31] Lorestani A, Ardehali MM. Optimal integration of renewable energy sources for autonomous tri-generation combined cooling, heating and power system based on evolutionary particle swarm optimization algorithm. Energy 2018;145:839–55. doi:10.1016/j.energy.2017.12.155.

[32] Zhou Z, Liu P, Li Z, Pistikopoulos EN, Georgiadis MC. Impacts of equipment off-design characteristics on the optimal design and operation of combined cooling, heating and power systems. Comput Chem Eng 2013;48:40–7. doi:10.1016/j.compchemeng.2012.08.007.

[33] Yang C, Yang Z, Cai R. Analytical method for evaluation of gas turbine inlet air cooling in combined cycle power plant. Appl Energy 2009;86:848–56. doi:10.1016/j.apenergy.2008.08.019.

[34] Ren H, Gao W, Ruan Y. Optimal sizing for residential CHP system. Appl Therm Eng 2008;28:514–23. doi:10.1016/j.applthermaleng.2007.05.001.

[35] Couper JR, Penney WC, Fair JR, Walas SM. Chemical Process Equipment, Selection and Design. Second Edi. USA: Elsevier; 2010.

[36] CEPCI historical trends. Available from: http://www.chemengonline.com/construction-cost-indices/?printmode=1 2018.

[37] Smith RM. Chemical Process Design and Integration. England: John Wiley & Sons Ltd; 2005.

[38] Richard E. Rosenthal. GAMS — A User's Guide. Washington, DC: GAMS Development Corporation; 2016.

[39] Zakrzewski T, Stephens B. Updated generalized natural gas reciprocating engine part-load performance curves for cogeneration applications. Sci Technol Built Environ 2017;23:1151–8. doi:10.1080/23744731.2016.1274623.

[40] Li H, Nalim R, Haldi PA. Thermal-economic optimization of a distributed multi-generation energy system - A case study of Beijing. Appl Therm Eng 2006;26:709–19. doi:10.1016/j.applthermaleng.2005.09.005.

List of Figure Captions

Figure 1. General superstructure and main decision variables for the trigeneration (combined heating, cooling and power – CHCP) system with thermal energy storage and bidirectional electricity grid connection. ICE, internal combustion engine; GFB, gas-fired boiler; TES, thermal energy storage; ACH, absorption chiller.

Figure 2. Different pricing scenarios generated from a multivariate Normal distribution by considering standard deviation of 20% from expected mean values (fuel price: 0.04 US$ $(kWh)^{-1}$ and electricity purchasing tariff: 0.12 US$ $(kWh)^{-1}$[†]) and: *(a)* matrix correlation factor of +0.1 (low-correlation); and, *(b)* matrix correlation factor of +0.8 (high-correlation).

Figure 3. Load duration curves for the electricity, heating and cooling demands for the hotel facility-reference case.

Figure 4. Distribution of the total annualized cost of the combined heating, cooling and power (CHCP) system throughout the different loading and pricing scenarios as obtained via the proposed stochastic approach. The red dashed line shows the expected value for the corresponding stochastic distribution, while the orange continuous line indicates the total annualized cost estimated by the deterministic model.

Figure 5. Distribution of the operating expenses of the combined heating, cooling and power (CHCP) system throughout the different loading and pricing scenarios as obtained via the proposed stochastic approach. The orange continuous line indicates the operating

[†]Cost data retrieved from the Eurostat database [28].

expenses estimated by the deterministic model. The distinct cost components of the operating expenses for the first 48 scenarios are shown in the zoomed in distribution.

Figure 6. Distribution of the thermal energy storage throughout the different loading and pricing (L&P) scenarios as obtained via the proposed stochastic approach.

Figure 7. Profiles for the: (*a*) electric power; and, (*b*) energy prices as obtained via the proposed stochastic approach. ICE, internal combustion engine.

Figure 8. Thermal power profiles as obtained via the proposed stochastic approach. ICE, internal combustion engine; GFB, gas-fired boiler.

Figure 9. Cumulative probability curves obtained for the optimal economic performance of the combined heating, cooling and power (CHCP) system by considering a low degree of correlation (+0.1) between energy prices. TAC, total annualized cost.

Figure 10. Cumulative probability curves obtained for the optimal economic performance of the combined heating, cooling and power (CHCP) system by considering a high degree of correlation (+0.8) between energy prices. TAC, total annualized cost.

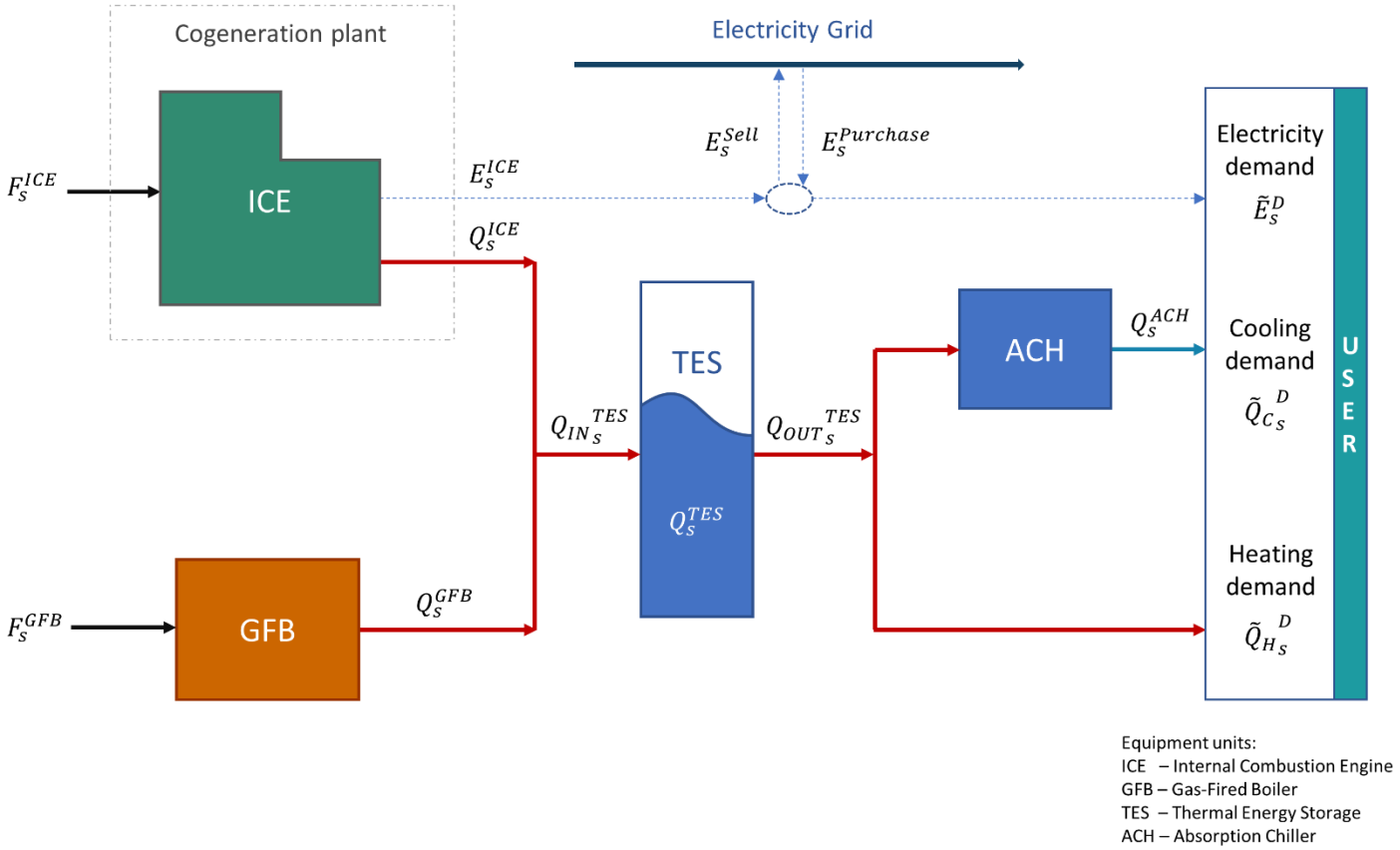

Figure 1. General superstructure and main decision variables for the trigeneration (combined heating, cooling and power – CHCP) system with thermal energy storage and bidirectional electricity grid connection. ICE, internal combustion engine; GFB, gas-fired boiler; TES, thermal energy storage; ACH, absorption chiller.

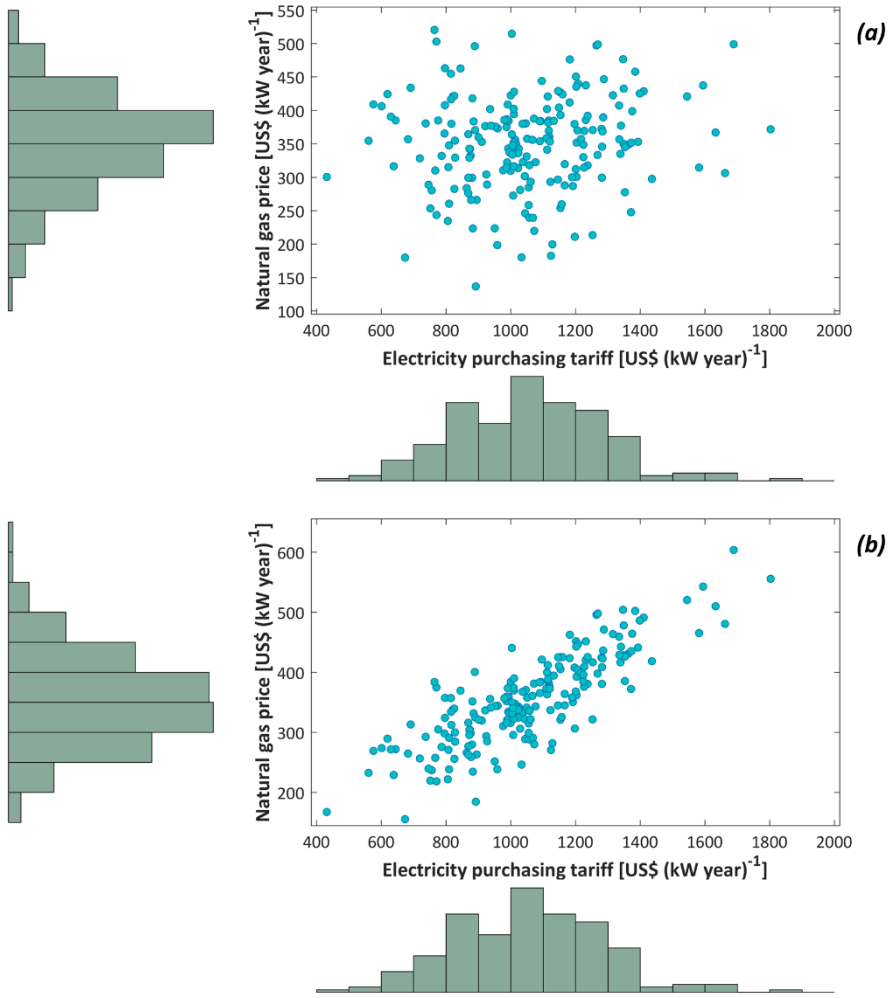

Figure 2. Different pricing scenarios generated from a multivariate Normal distribution by considering standard deviation of 20% from expected mean values (fuel price: 0.04 US$ (kWh)$^{-1}$ and electricity purchasing tariff: 0.12 US$ (kWh)$^{-1}$‡) and: *(a)* matrix correlation factor of +0.1 (low-correlation); and, *(b)* matrix correlation factor of +0.8 (high-correlation).

‡Cost data retrieved from the Eurostat database [28].

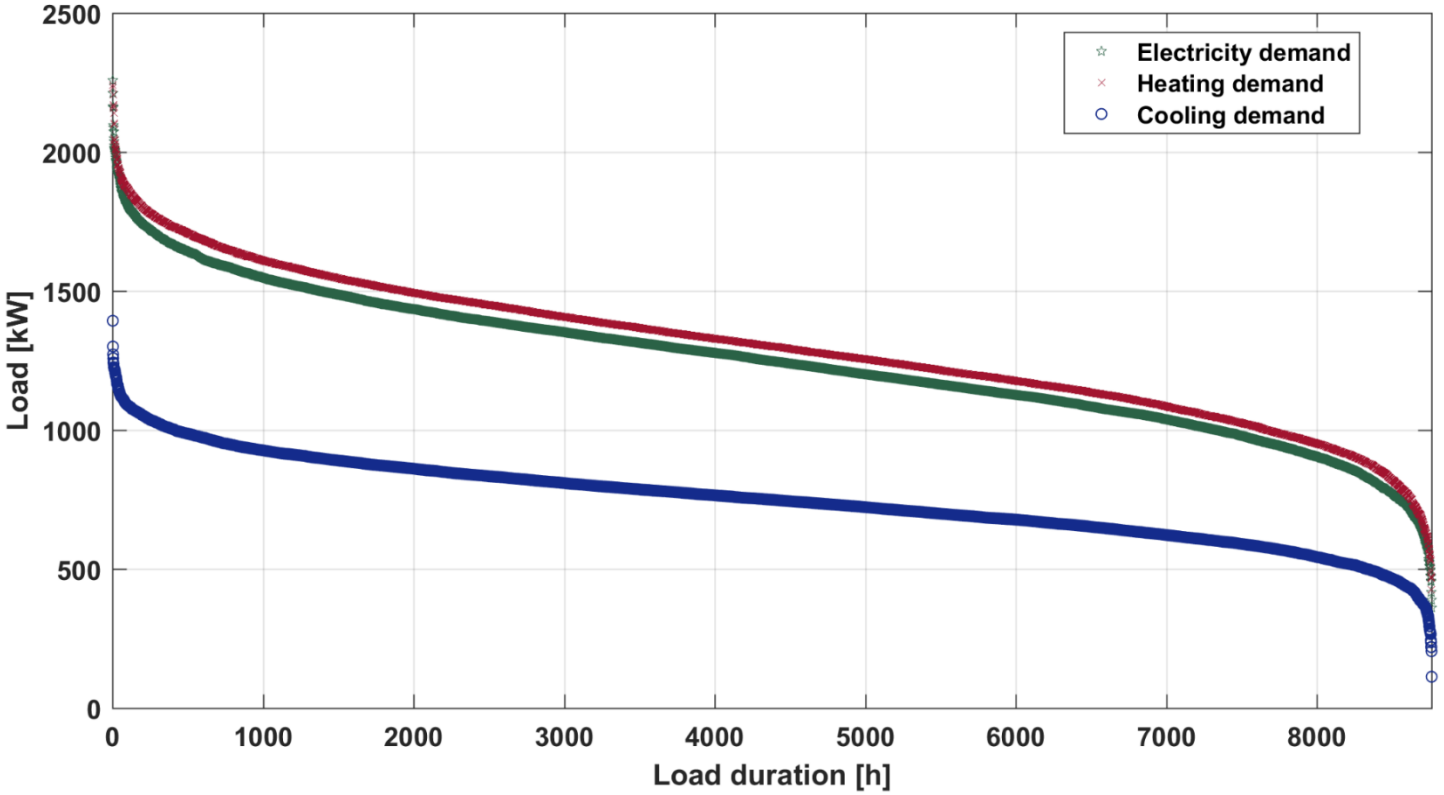

Figure 3. Load duration curves for the electricity, heating and cooling demands for the hotel facility-reference case.

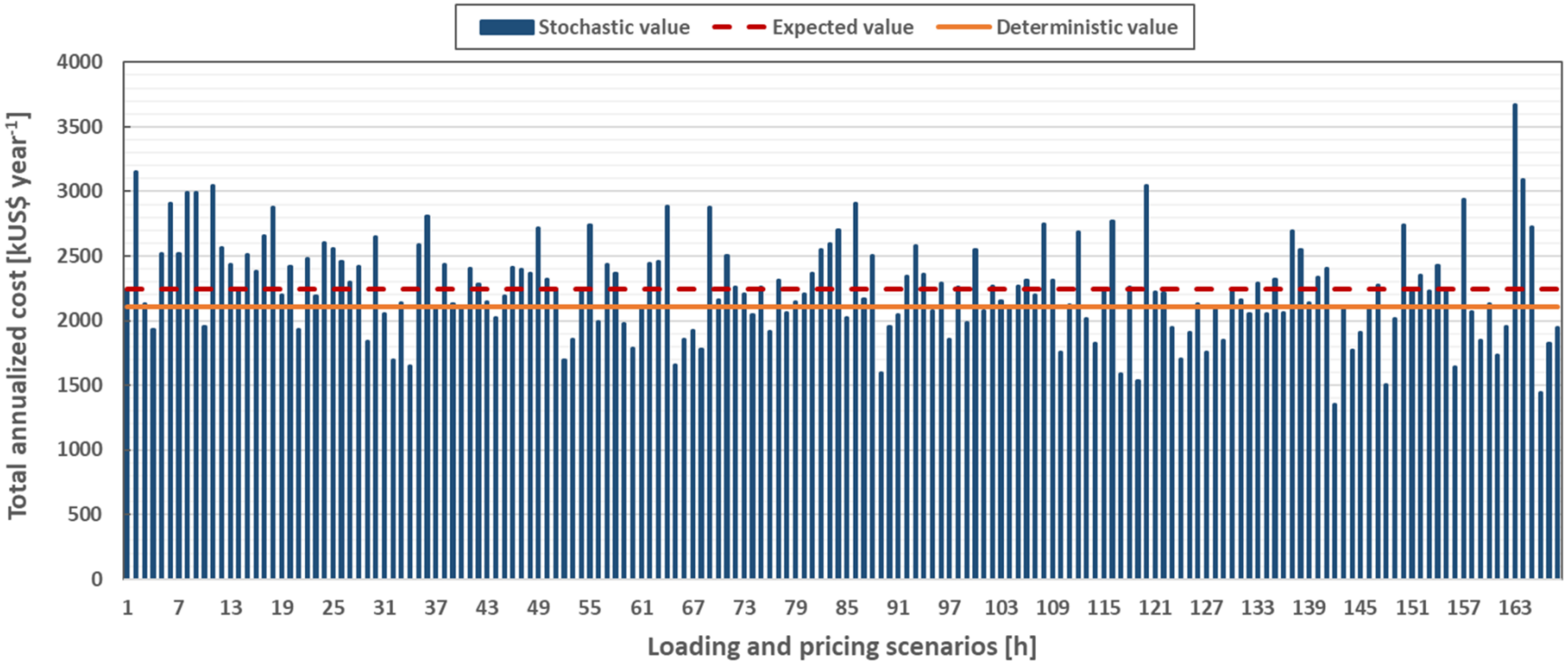

Figure 4. Distribution of the total annualized cost of the combined heating, cooling and power (CHCP) system throughout the different loading and pricing scenarios as obtained via the proposed stochastic approach. The red dashed line shows the expected value for the corresponding stochastic distribution, while the orange continuous line indicates the total annualized cost estimated by the deterministic model.

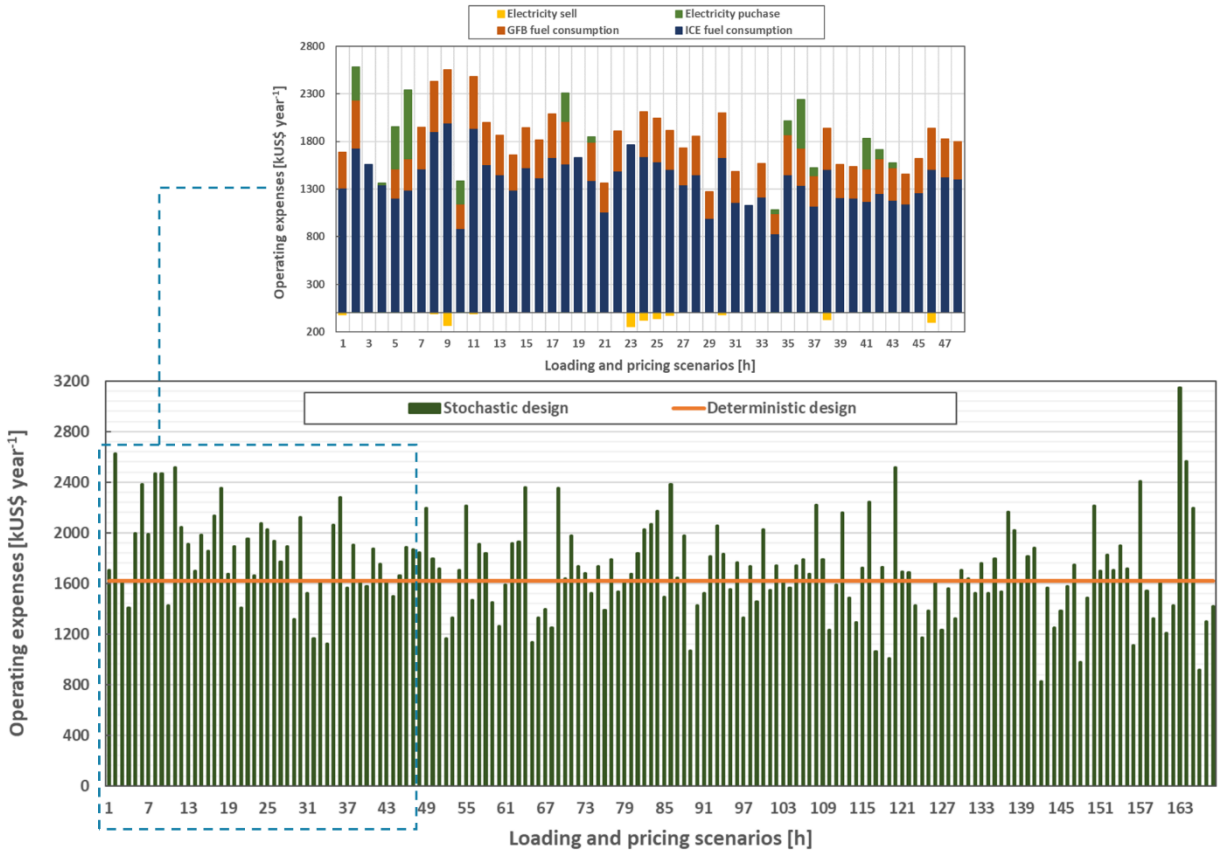

Figure 5. Distribution of the operating expenses of the combined heating, cooling and power (CHCP) system throughout the different loading and pricing scenarios as obtained via the proposed stochastic approach. The orange continuous line indicates the operating expenses estimated by the deterministic model. The distinct cost components of the operating expenses for the first 48 scenarios are shown in the zoomed in distribution.

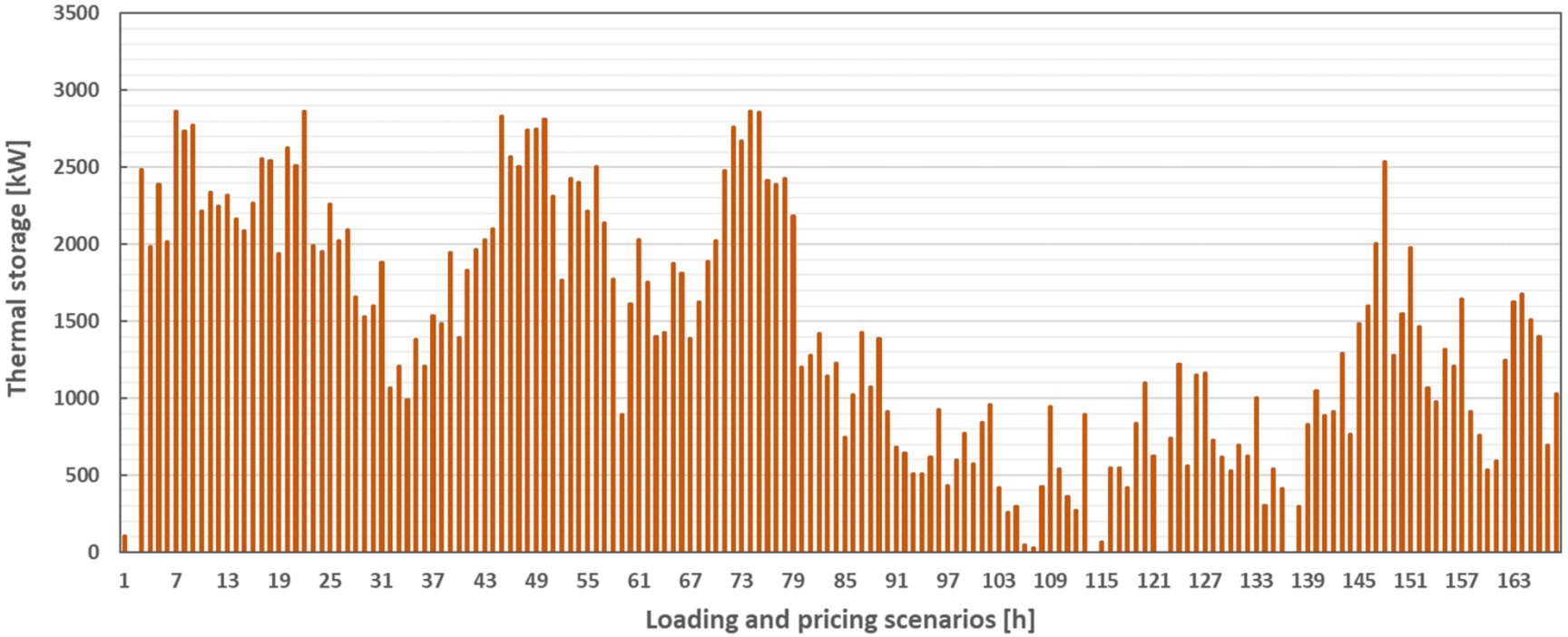

Figure 6. Distribution of the thermal energy storage throughout the different loading and pricing (L&P) scenarios as obtained via the proposed stochastic approach.

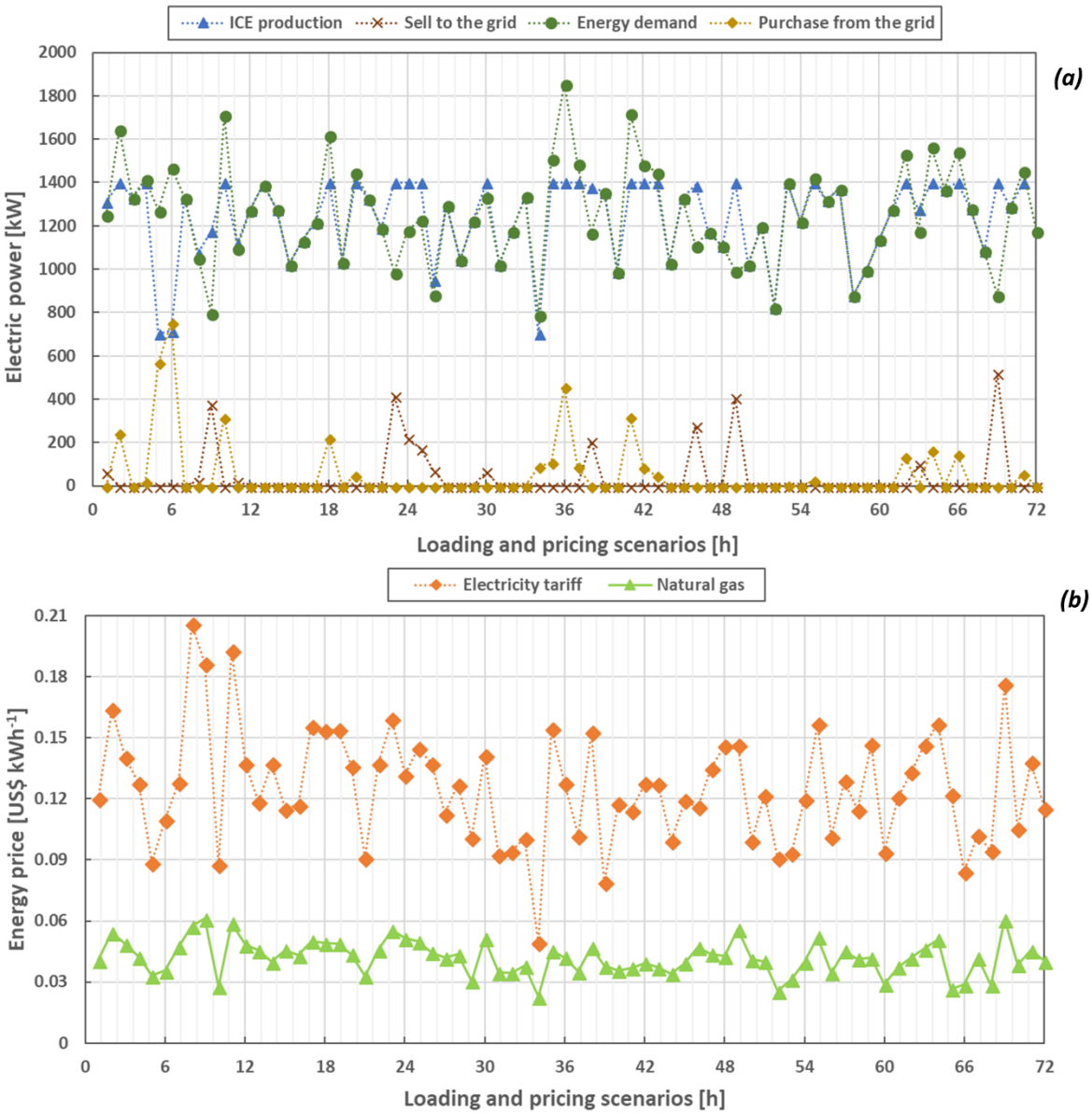

Figure 7. Profiles for the: (*a*) electric power; and, (*b*) energy prices as obtained via the proposed stochastic approach. ICE, internal combustion engine.

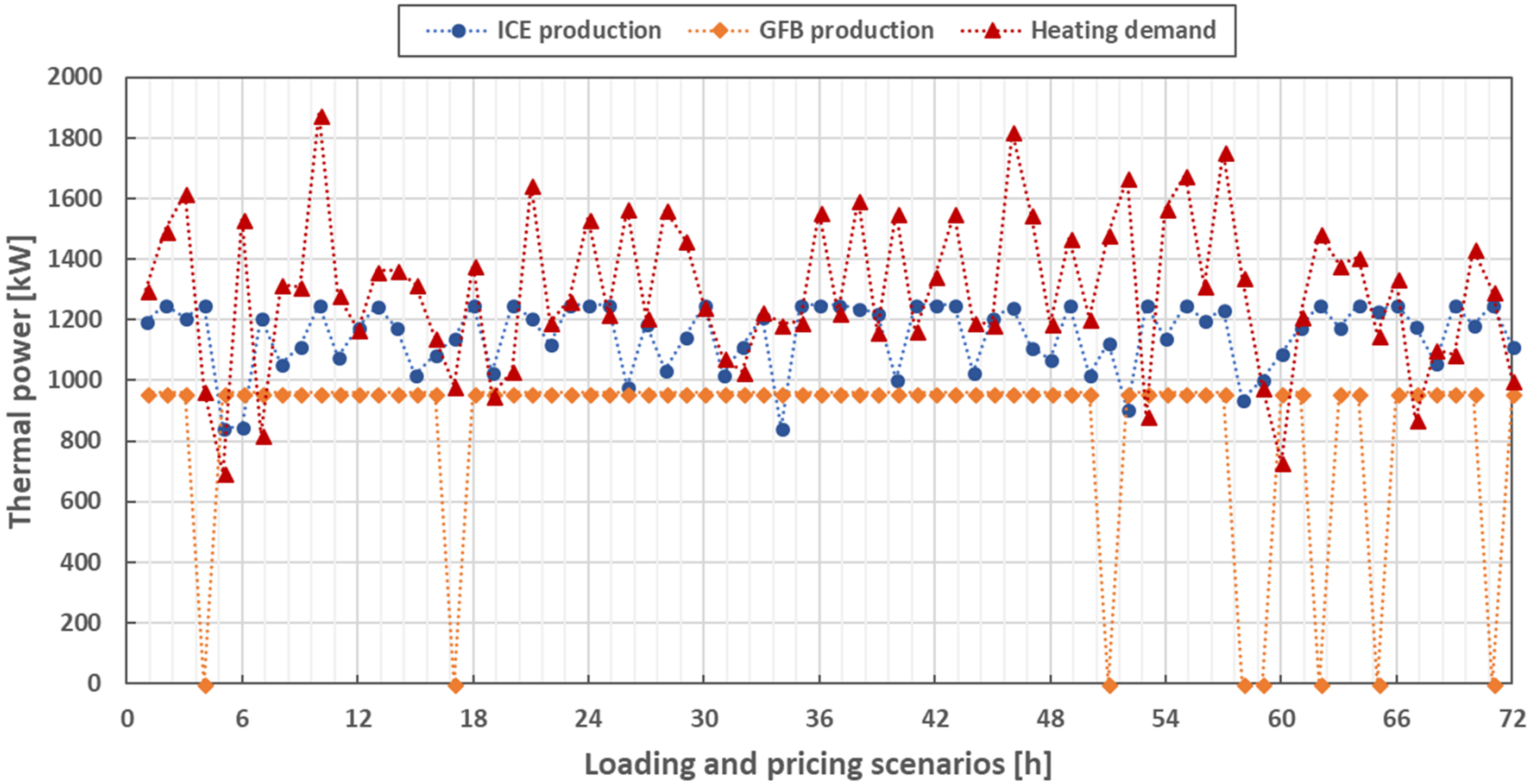

Figure 8. Thermal power profiles as obtained via the proposed stochastic approach. ICE, internal combustion engine; GFB, gas-fired boiler.

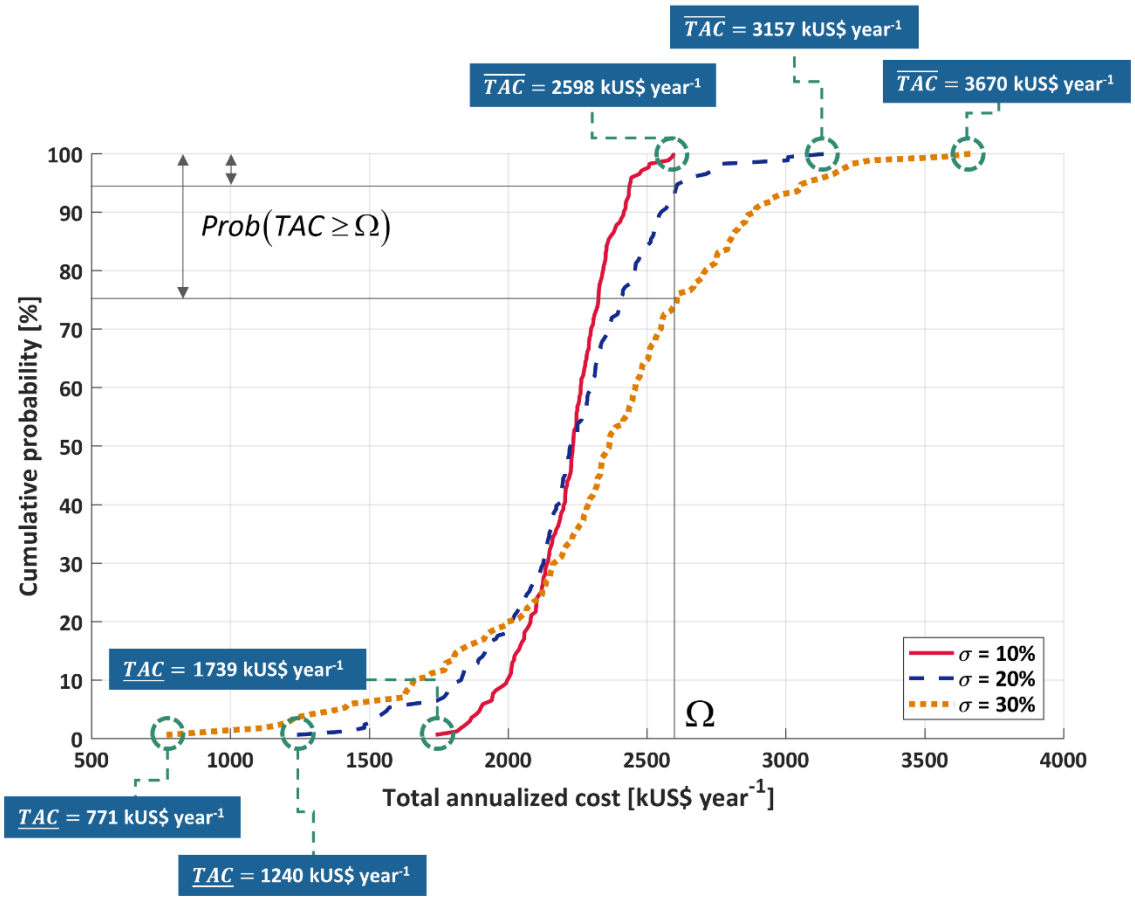

Figure 9. Cumulative probability curves obtained for the optimal economic performance of the combined heating, cooling and power (CHCP) system by considering a low degree of correlation (+0.1) between energy prices. TAC, total annualized cost.

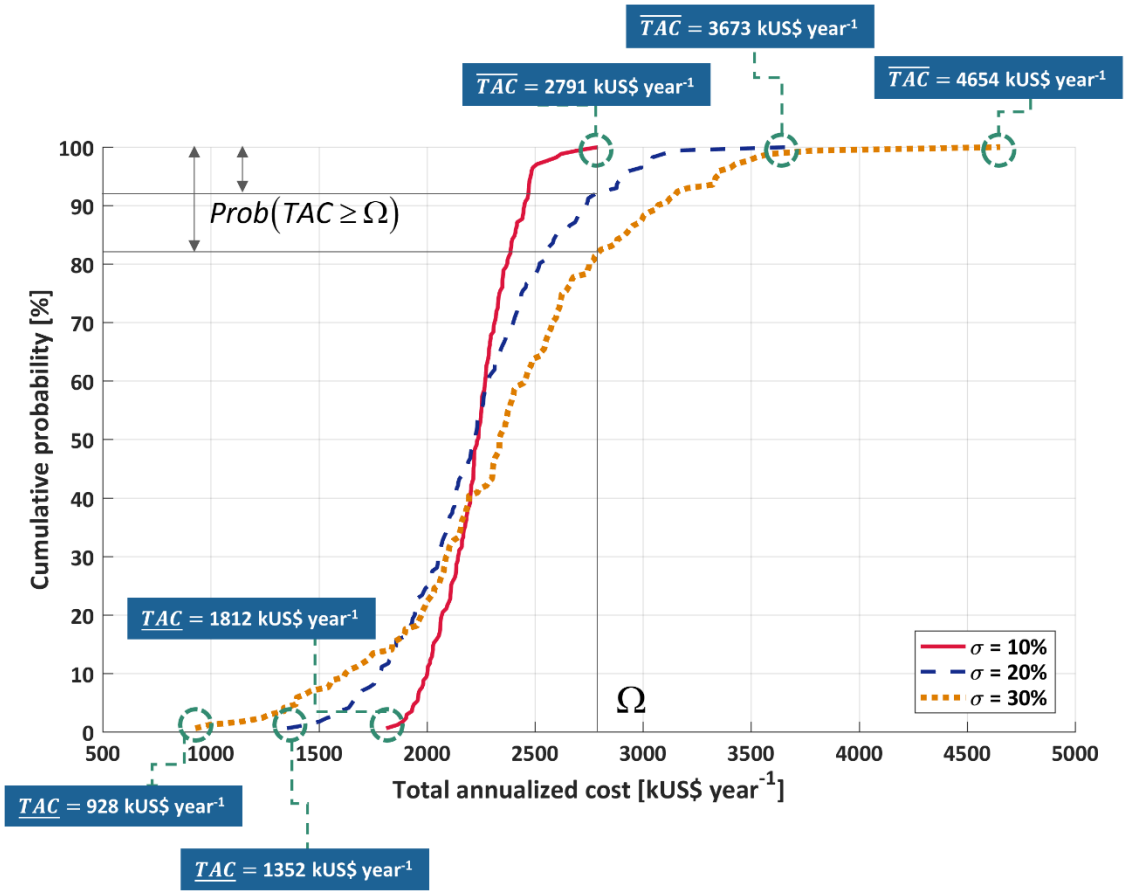

Figure 10. Cumulative probability curves obtained for the optimal economic performance of the combined heating, cooling and power (CHCP) system by considering a high degree of correlation (+0.8) between energy prices. TAC, total annualized cost.

Table 1

Part-load performance characteristics of the different equipment used in the trigeneration system.

Technology	Part-load performance curve	Reference
ICE	▪ Electrical efficiency: $\eta_{Ei,s}^{ICE} = \eta_{E,N}^{ICE} \cdot \left(1.1260 \cdot LF_{i,s}^{ICE} - 0.1260\right)$ ▪ Thermal efficiency: $\eta_{Qi,s}^{ICE} = \eta_{Q,N}^{ICE} \cdot \left(0.8253 \cdot LF_{i,s}^{ICE} + 0.1747\right)$ ▪ Partial load factor: $LF_{i,s}^{ICE} = \eta_{Ei,s}^{ICE} \cdot F_{i,s}^{ICE} \big/ W_i^{ICE}$	[8,39]
GFB	▪ Thermal efficiency: $\eta_{i,s}^{GFB} = \eta_N^{GFB} \cdot \left[0.0951 + 1.525 \cdot LF_{i,s}^{GFB} - 0.6249 \cdot \left(LF_{i,s}^{GFB}\right)^2\right]$ ▪ Partial thermal load factor: $LF_{i,s}^{GFB} = Q_{i,s}^{GFB} \big/ QR^{GFB}$	[32,40]
ACH	▪ Thermal consumption: $QC_{i,s}^{ACH} = C_{LFi,s} \cdot C_{\overline{T}} \cdot Q_R^{ACH}$ ▪ Correction coefficients: $\begin{cases} C_{LFi,s} = \left[\begin{array}{l} 0.015 + 1.24 \cdot LF_{i,s}^{ACH} - 0.915 \cdot \left(LF_{i,s}^{ACH}\right)^2 \\ +0.66 \cdot \left(LF_{i,s}^{ACH}\right)^3 \end{array}\right] \\ C_{\overline{T}} = 0.987 - 0.689 \cdot \overline{T} + 0.702 \cdot \overline{T}^2 \end{cases}$ ▪ Partial thermal load factor: $LF_{i,s}^{ACH} = Q_{i,s}^{ACH} \big/ QR^{ACH}$	[1,32]

ICE, internal combustion engine; GFB, gas-fired boiler; ACH, absorption chiller.

Table 2

Design parameters for the different equipment units used in the trigeneration system [8,31,32].

Technology	Parameter	Symbol	Value [Unit]
ICE	Nominal electrical efficiency	$\eta_{E,N}^{ICE}$	0.385 [-]
	Nominal thermal efficiency	$\eta_{Q,N}^{ICE}$	0.344 [-]
	Nominal capacity	W_i^{ICE}	600 – 1600 [kW]
GFB	Rated thermal efficiency	η_N^{GFB}	0.9 [-]
	Rated thermal capacity	$Q_R{}^{GFB}$	960 [kW]
TES	Thermal efficiency	η^{TES}	0.9 [-]
ACH	Rated performance coefficient	COP_R^{ACH}	1.24 [-]
	Rated thermal capacity	Q_R^{ACH}	1300 [kW]

ICE, internal combustion engine; GFB, gas-fired boiler; TES, thermal energy storage; ACH, absorption chiller.

Table 3

Economic evaluation data considered in the case study.

Parameter	Symbol	Value [Unit]
Electricity purchasing tariff (expected mean value) *	$\tilde{C}_s^{Ptariff}$	0.12 [US$ (kWh)$^{-1}$]
Electricity selling tariff	$C^{Stariff}$	0.04 [US$ (kWh)$^{-1}$]
Natural gas cost (expected mean value) *	$\tilde{C}_s^{NG}$	0.04 [US$ (kWh)$^{-1}$]
Fractional interest rate per year	fi	0.1 [-]
Amortization period	t	10 [years]
Working hours per year	-	8760 [h]

* Cost data obtained from the Eurostat database [28].

Highlights

New stochastic model to optimize trigeneration systems under long-term uncertainties.

Loading and pricing scenarios are generated via Monte Carlo-based sampling technique.

Uncertain loads and prices significantly affect the energy and economic performances.

Economic risk analysis reveals riskier decision-making for higher uncertainty levels.

Higher correlations between the energy prices can also imply riskier decision-making.